Table of Contents for Chapter 5

5.1 Introduction 2
5.2 Research Plans 5
5.2.1 Thrust MP-1: Understand lithium surface-science for long-pulse PFCs 5
5.2.1.1 Research Plans by Year for Thrust MP-1 12
5.2.1.2 Baseline Deliverables for Thrust MP-1 15
5.2.1.3 Incremental Funding Research Plans and Deliverables 15
5.2.2 Thrust MP-2: Unravel the physics of tokamak-induced material migration and evolution 15
5.2.2.1 Research Plans by Year for Thrust MP-2 24
5.2.2.2 Baseline Deliverables for Thrust MP-2 26
5.2.2.3 Incremental Funding Research Plans and Deliverables 26
5.2.3 Thrust MP-3: Establish the science of continuous vapor-shielding 27
5.2.3.1 Research Plans by Year for Thrust MP-3 32
5.2.3.2 Baseline Deliverables for Thrust MP-3 33
5.2.3.3 Incremental Funding Research Plans and Deliverables 33
5.3 Plasma-Facing Component Research & Development 34
5.3.1 Staged Solid PFC Upgrades 36
5.3.2 Liquid-Metal Plasma-Facing Component Research and Development 38
5.4 Theory and Modeling 40
5.4.1 Materials & Atomic Physics 40
5.4.1.1 Monte Carlo Plasma-Surface Interaction Simulations 40
5.4.1.2 Molecular Dynamics Codes 41
5.4.1.3 Atomic Data and Analysis Structure Database 41
5.4.1.4 Surface Chemistry and Evolution Modeling 42
5.4.1.5 Global Transport and Evolution Simulations 43
5.4.1.6 1-D Modeling of Mixed-Material Films 45
References 46

Chapter 5

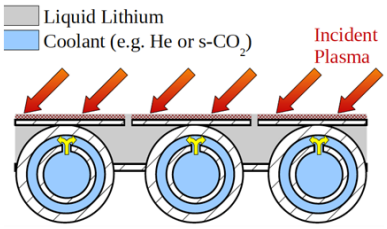

Research Goals and Plans for Materials and Plasma-Facing Components

5.1 Introduction

As described in other chapters of this 5 year plan, substantial progress has been made in producing and controlling stable high-performance ST plasmas with energy confinement at or near levels needed for a next-step facility such as a fusion nuclear science facility (FNSF) [*c.f.* Chapter 1]. A major remaining challenge for NSTX-U and other magnetic fusion devices generally is to extend high-performance plasmas for very long durations, and to integrate this high performance with plasma facing components (PFCs) that can withstand very high heat and particle fluxes while maintaining structural integrity with minimal retention of fusion fuel in a harsh nuclear environment. The present frontrunner material considered in reactor studies to have the best hope of meeting these substantial challenges consists of PFCs composed of a solid refractory metal, typically tungsten or its alloys [1]. As recent reports point out, there are significant uncertainties as to whether tungsten will, ultimately, extrapolate to an economically viable fusion reactor. Several failure modes exist that will force regular component replacement due to erosive fluxes as well as replacement in the case of significant transient events that would cause melting (e.g. disruptions or large ELMs). Given the critical nature of the PFC materials question to the fusion enterprise on a whole, it is prudent to consider, and provide clear comparisons with, alternative technologies when looking at the challenges associated with FNSF and DEMO [2].

An alternative to solid PFCs are those composed of liquid metals (LM PFCs). The most commonly considered metals for this purpose are lithium, tin and gallium. The most intriguing

potential for a LM PFC is that of self-healing which would eliminate both net erosion effects (extending component lifetimes against this damage mechanism) and the effects of transient disruptions as liquid surfaces will simply return to equilibrium positions after an event. These traits are shared by all of the liquid metals. While potential is great, however, LM PFCs raise new issues for both the science and technology associated with this innovative option.

The NSTX-U device [3] will provide unique opportunities for research on both solid and liquid PFCs. With a major radius of only 0.93m and maximum heating power of 19.2MW, NSTX-U will have one of the largest P/R ratios in the world as well as a significant P/S ratio (where P is the heating power, R is the major radius and S is the surface area of the last-closed flux surface). Table 5.1 shows a comparison of NSTX-U projected maximum parameters and those from other machines worldwide in the recent multi-machine heat-flux width database [4] as well as projections to an FNSF based on the ST-Pilot and an ST-DEMO [5] (only maximum heating power for the NSTX-U is provided at this time until more accurate assessments of radiated power fraction are available). High-power density devices present two challenges, the first obviously being reduction of exhaust power to acceptable levels. The second challenge is the ability to handle steady erosive fluxes caused by plasma-material interactions within the vessel.

Table 5.1: Multi-machine comparison of size and various power-exhaust metrics. ST-Pilot and ST-DEMO pulse lengths given in terms of discharge-seconds per year.

Machine	R_0 [m]	$P_{SOL}(P_{AUX})$ [MW]	P/R [MW/m]	P/S [MW/m^2]	τ_{pulse} [s]
NSTX*	0.86	6.8	8	0.2	1
NSTX-U*	**0.93**	**19**	**21**	**0.6**	**5**
JET†	2.95	12 (35)	4.1 (12)	0.03 (0.2)	20
DIII-D†	1.74	5 (20)	2.9 (11)	0.1 (0.4)	6
AUG†	1.65	5 (27)	3 (16)	0.1 (0.6)	10
CMOD†	0.7	3 (6)	4 (9)	0.4 (0.7)	2
MAST†	0.87	5 (7.5)	6 (9)	0.2 (0.25)	1
ITER†	6.2	100	16	0.15	400
ST-Pilot‡	**2.2**	**190**	**86**	**0.7**	6×10^6
ST-DEMO‡	**3.2**	**520**	**161**	**0.9**	∞

* J.E. Menard, *et al.*, Nucl. Fusion **52** (2012) 083015.

† Th. Eich, *et al.*, "Scaling of the tokamak near scrape-off layer H-mode power width and implications for ITER", ITPA-Div/SOL group ITR 1/1, San Diego, October, 2012.

‡ J.E. Menard, *et al.*, Nucl. Fusion **51** (2011) 103014.

These issues are being addressed in the NSTX-U program via multiple routes. In the Boundary Physics plan in Chapter 4, advanced divertor magnetic configurations (e.g. snowflake) and radiative power exhaust are being examined for heat-flux mitigation. In the Materials and PFCs Topical Science Group (M&P TSG), the concept of the continuously vapor-shielded PFC is being examined to reduce power incident on the divertor target itself. In the case of eliminating or controlling erosion and material transport, the long-range concept of liquid-metal PFCs is being pursued in NSTX-U. This work will begin the assessment of high-Z metal PFCs versus liquid lithium PFCs through a systematic conversion of the NSTX-U. This comparison will provide important data informing the use of either technology in future devices. High-Z materials, which are important to study in their own right, are also ultimately needed to provide a fusion-relevant solid substrate to support flowing liquid metals.

Current plans are to begin operations with carbon PFCs in NSTX-U and gradually transition to high-Z PFCs with increasing emphasis on the liquid-metal PFC option (see research timelines at end of this chapter). This transition presents unique research opportunities for both solid- and liquid-PFC research. Over the next 5-years the M&P TSG will undertake three thrusts: (1) Understand lithium surface-science for long-pulse PFCs, (2) Unravel the physics of tokamak-induced material migration and evolution and (3) Establish the science of continuously vapor-shielded plasma-facing components.

Significant progress in liquid-metal technology is required before a flowing-liquid metal module can be implemented in NSTX-U. Ongoing work in understanding the science of liquid metal surfaces and in developing these PFCs will be described. In the incremental budget scenario, such a fully-flowing liquid metal module might be installed in the NSTX-U by the end of the 5-year period. Further, in the incremental budget scenario, a substantial fraction of the first-wall (in low heat-flux regions) will be coated with high-Z materials to accelerate assessments of the ability to integrate high-performance ST plasmas with a high-Z first-wall. Significant progress can still be made in understanding the physics associated with such PFCs even in the baseline budget plan.

Three research thrusts for the NSTX-U Materials and Plasma-Facing Components group are proposed for this 5 year plan with the following thrust titles: Understand Lithium Surface Science for Long-Pulse PMI and PFCs, Unravel the Physics of Tokamak-Induced Material Migration and Evolution, and Establish the Science of Continuous Vapor Shielding The motivation and research strategy for each thrust are provided in Section 5.2 of this document. The solid and liquid plasma-facing component research and development required to implement the staged NSTX-U upgrade is provided in Section 5.3. Finally, supporting theory and modeling tools are described in Section 5.4.

5.2 Research Plans

5.2.1 Thrust MP-1: Understand lithium surface-science for long-pulse PFCs

Lithium research to date on the NSTX has focused on the usage of this material as a wall-condioning tool. This work has demonstrated increases in discharge performance and is also key contributions toward understanding how the wall-conditioning is affecting the PFCs. However, there remain key questions, particularly in the area of what role impurities in the lithium (e.g. boron, oxygen and carbon) affect the coating performance, and how this performance will change when lithium is applied to a high-Z substrate. The purpose of this thrust is to improve the understanding of this wall conditioning method and what other variables may be impacting performance through a combination of tokamak experimental studies and surface-science laboratory studies. These considerations motivate the following research thrust:

> **Thrust MP-1:** *Experiments will be conducted to improve understanding of the role of more complete coverage of the PFCs by evaporated lithium using upward-facing evaporators and/or diffusive evaporation as well as the impact of boronization. A boronization campaign in year one will be followed by a controlled Li introduction. The Materials Analysis Particle Probe (MAPP) will be utilized to identify in-situ between-shot chemical states and compositions of the coatings. The total deposited lithium as supplied in 2008 will be applied on both upper and lower divertors. The changes in plasma performance will be compared to the 2008 database. In the second year, a boronization campaign will be eliminated and an identical introduction of lithium as in the previous year will be applied to bare graphite surfaces. These studies will provide a comparison between C+B substrate vs. a C substrate alone in terms of plasma performance. The MAPP diagnostic will be utilized during this year also, and will enable comparisons to surface-science laboratory results including Li-coatings on high-Z metal substrates such as TZM. The uptake of hydrogenic species and the impact of varying levels of impurities (e.g. C, O) on that uptake will be examined in the Li-metal system, and in years 3-5 the surface interactions of Li on high-Z tiles in at least one NSTX-U divertor region will be studied.*

This section will describe recent developments in the surface characteristics of lithium coatings as well as recent analysis of the effect of lithium wall conditioning on global energy confinement in NSTX. The question of surface purity is highlighted, however, in additional results examining the Liquid Lithium Divertor experiments which did not demonstrate large changes in global energy confinement. The section ends with a description of the detailed research plans expected

to be undertaken in the baseline funding scenario as well as the results expected by the end of the 5-year plan.

The efficacy of lithium PFCs in improving plasma performance was demonstrated on TFTR, CDX-U, T-11M, and other devices prior to lithium evaporation on carbon PFCs in NSTX [12]. On NSTX, there was a concern that the intercalation of the lithium into the carbon would affect its effectiveness as a PFC coating [13]. Instead, NSTX plasmas with lithium-coated PFCs showed higher energy confinement, ELM suppression, and other examples of plasma improvement over discharges with carbon PFCs alone [14]. The research strategy employed here is to understand the changes in surface composition and chemistry at the microscopic scale and link that to overall machine performance. In addition to on-site and collaborator surface-science laboratories, the Material-Analysis and Particle Probe (MAPP) is also a key tool for linking the in-vessel conditions with those that can be studied in a controlled laboratory setting. This diagnostic essentially allows us to identify what changes are occurring when lithium "conditions" the surface of the PFCs and how the plasma interactions change this surface.

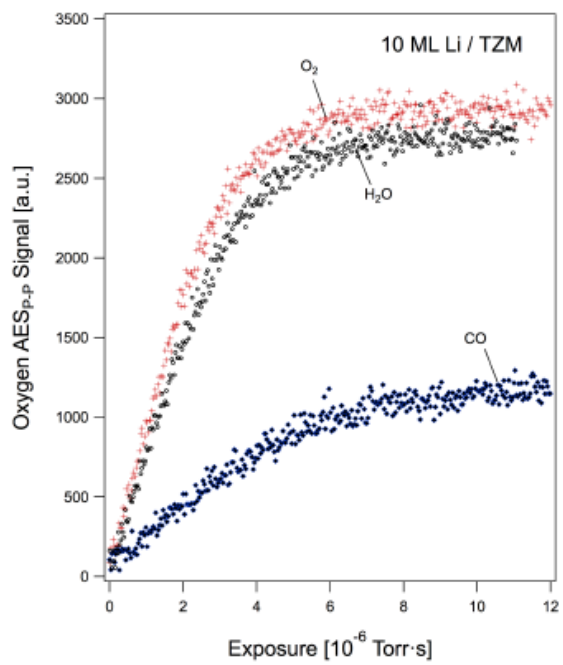

Figure 5.1: Auger electron signal shows that Li film oxidizes in 100s at $1x10^{-7}$ Torr of water vapor. If Li film is not replenished between shots in NSTX, the plasma will see a mixed material, not a pure Li coating[6].

To take advantage of the benefits of lithium or other liquid metals plasma facing components (PFCs) and provide a design basis for next-step PFCs, it is important to develop a database of measurements on the behavior of lithium / liquid metal surfaces in response to the conditions found at the PFCs within the tokamak. Many of the key processes are amenable to investigation in laboratory experiments where the full range of modern surface analysis equipment may be brought to bear on investigating the atomic-scale details of the chemical composition of solid and liquid liquid metal surfaces and their interactions with plasma constituents and residual gases in well characterized conditions. The results will advance the scientific understanding of plasma-lithium surface interactions, aid the development of liquid metal plasma facing components with superior performance for long-pulse discharges, and provide the pathway to advanced PFCs for FNSF.

Two new laboratories for materials characterization and surface chemistry experiments have been established at PPPL (see also chapter 10, section 10.5.2.9). These contain four distinct surface analysis instruments that interrogate and image surfaces in multiple and complementary ways with ions, electrons and x-rays in controlled UHV conditions. One instrument has applied Auger electron spectroscopy to demonstrate that lithium surfaces react on short time-scales with residual gases such as water and oxygen (Fig. 5.1, [6]). At a partial pressure of water similar that in NSTX, a monolayer of oxide forms on a lithium surface in a time shorter than the inter-discharge time of 600s, thus the NSTX plasma interacts with lithium oxide and not metallic lithium. This work also showed how the surface composition in future flowing Li-PFC systems will depend on residual vacuum pressure and Li flow rate.

Joining surface-science tools and modeling with plasma-facing components has already yielded unexpected findings and increased the understanding of lithium wall conditioning in NSTX. Detailed surface analysis of PFC samples removed from NSTX after run periods indicated that lithium did indeed alter the morphology of the carbon surfaces, but in a way that improved its ability to retain deuterium [15]. Quantum-classical molecular dynamic (QCMD) simulations showed how the interaction of the lithium with the carbon created brought oxygen to the surface, and made it a key factor in binding deuterium [16]. These computational studies were guided, in part, by previous analysis of PFC samples, it is, however, advantageous to study these surface in vacuo to avoid any possibility of contamination by atmospheric gases.

The MAPP [17] is a novel surface analysis capability that will contribute to the study of in-situ NSTX PFC materials. MAPP has the ability to expose samples to NSTX plasmas, and withdraw them immediately after a discharge for in-vacuo surface analysis in an attached chamber with multiple diagnostics. This in-vacuo analysis capability is important as lithium surfaces are highly reactive to air. The MAPP system is able to apply thermal desorption spectroscopy (TDS), x-ray photoelectron spectroscopy (XPS) and low-energy ion scattering spectroscopy (LEISS) to samples immediately following exposure to tokamak discharges. The system is described in more detail in Chapter 10 (Section 10.6.4.1) and Chapter 11 (Section 11.2.17).

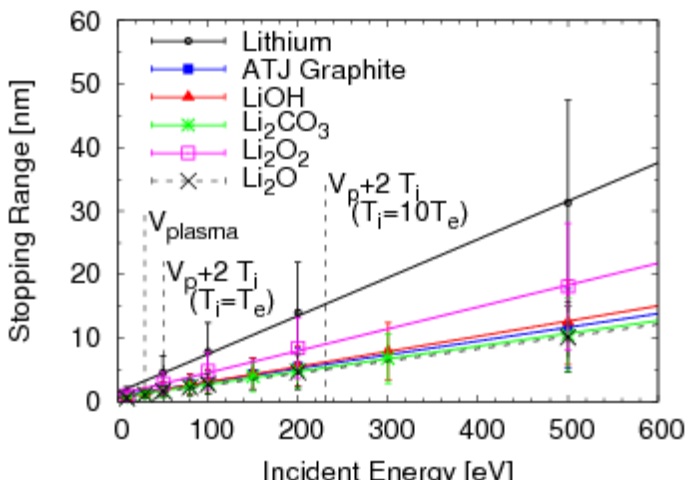

Figure 5.2: Stopping ranges of deuterium ions in pure lithium or a mixed-material surface as a function of incident energy [8].

Surface science studies in the laboratory have already indicated that lithium surfaces react on short time-scales with residual gases such as water and oxygen. Referring again to Figure 5.1, measurements were made of oxygen uptake using Auger-Electron Spectroscopy [6]. A typical inter-discharge base pressure inside the NSTX vacuum vessel is about 10^{-7} Torr. At partial pressures similar to this of oxygen or water, a monolayer of oxide would be expected to form on the lithium surface in about 100-200s. This time is already comparable to the inter-discharge time of 600s. The existence of the mixed-material surface leads to obvious questions in relating results in NSTX with previously published studies in linear machines, such as PISCES-B, where removal of contaminants was performed before studies of deuterium uptake [7]. Given the short time-scales involved, this provides a clear example of how MAPP will provide a link between in-vessel conditions with those reproduced in the laboratory setting. With a combination of XPS, DTS and LEISS, MAPP will be able to characterize the surface of the PFC before and after discharges. These characterizations will provide key metrics that will enable other surface-science laboratories to mimic the in-vessel conditions.

Plasma interactions with contaminated and uncontaminated surfaces are expected to be sensitive to the first 10 nanometers of material. Simple TRIM estimates of implantation depth are shown in Fig. 5.2. This small amount of lithium available for interaction must be considered with observations that the improvement in confinement during lithium deposition experiments improves with increasing deposition quantities. Figure 5.3 shows the deposited lithium in the NSTX vessel during a dedicated experiment in the 2008 run campaign; no lithium was injected before this experiment in 2008. The approximate surface area for deposition is $2m^2$ on the lower divertor floor.

With this areal coverage, every milligram of deposited lithium results translates to about 1nm of depth on the lower PFCs. That is, the initial deposition of a little more than 100 mg should provide a nominal 100nm of lithium on average in the lower divertor – well in excess of the implantation depth. Despite these estimates, it was found that the discharge performance continuously improves with increasing quantities of lithium. Figure 5.4 shows the evolution of plasma performance as a function of the pre-discharge lithium deposition quantity.

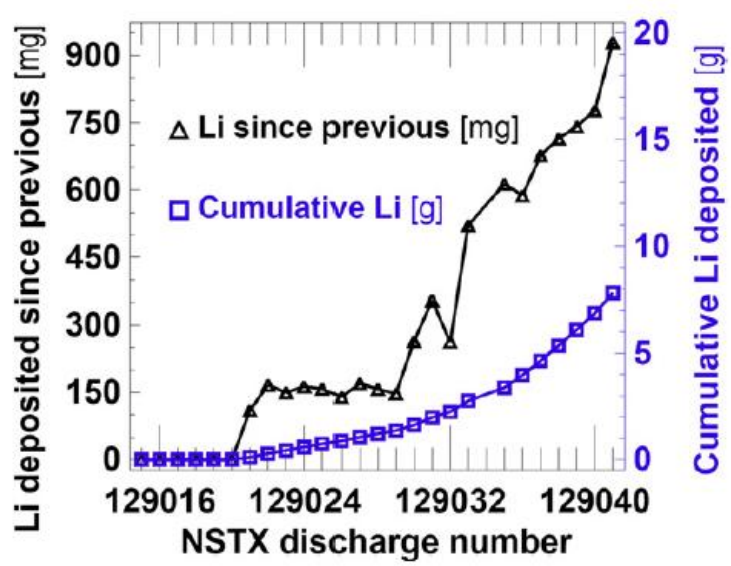

Figure 5.3: Lithium deposition during the systematic introduction of lithium during the FY 2008 run campaign[9].

It can be seen that during this scan, panel 4(d) shows a nearly continuous improvement in the confinement factor from an H97-L factor of ~1.6 as much as 3 with increasing amounts of lithium.

The role of gettered oxygen from residual gases vs oxygen migrating to the surface from the graphite substrate remain open questions, as does the role of plasma-induced redistribution of lithium during operations. This highlights the importance of a multi-pronged approach to understanding the lithium surface-science and it's relation to global tokamak discharge performance.

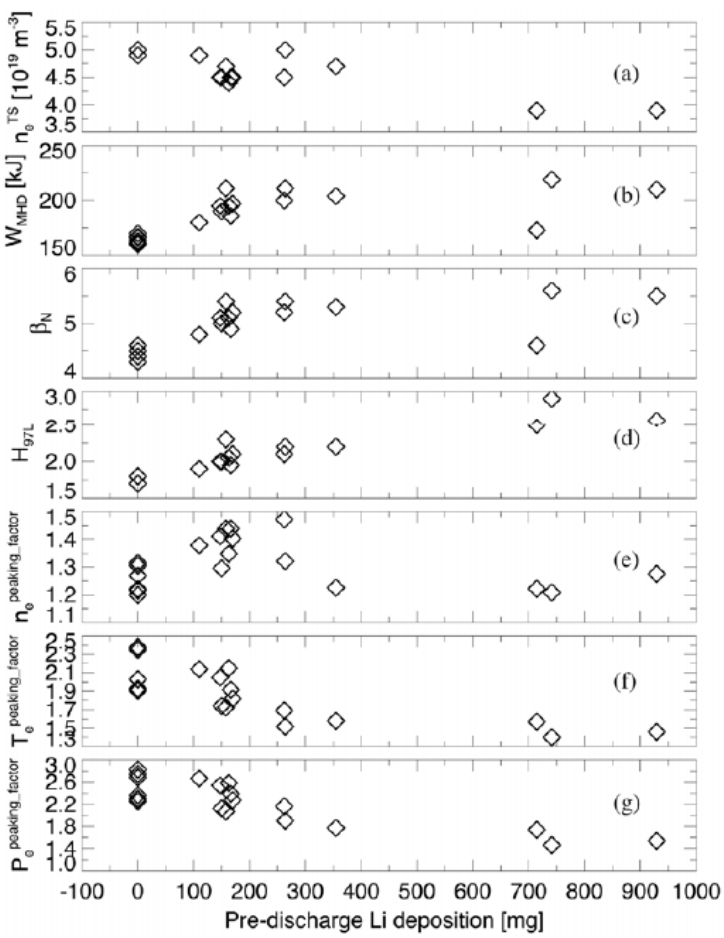

Figure 5.4: Evolution of plasma parameters and profile peaking during the systematic scan shown in Fig. 5.2.1.3. Panel (d) shows the H-factor for confinement relative to the ITER97-L scaling at the time of the peak stored energy. All discharges were operated with 4MW injected NBI except for the final three with the highest Li evaporation which had P_{NBI}=2, 3, 3 MW respectively [9].

The results shown in ref. [8] can be contrasted with those obtained with the liquid lithium divertor (LLD) experiments of FY2010 (see [18] for a description of NSTX operations with the LLD). In this run campaign, no boronization was performed, but operations began after an initial deposition of 15g of lithium onto the lower divertor of NSTX. Discharges on the LLD showed remarkable similarity throughout the run-year, despite the increasing accumulation of in-vessel lithium. Experiments in FY 2010 did not, however, include a dedicated scan of lithium deposition rate (analogous to pre-discharge lithium in fig. 5.3) and this motivates additional studies during this 5-year plan period. An investigation of the relative emission of impurities from the divertor region is shown in Figure 5.5. In this figure the top three panels show the relative emission as a function of strike-point radius during experiments diverted in the vicinity of the LLD. The transition between the graphite tiles and LLD occurs at 0.65m (graphite is inside of

0.65m radius). The emission from the divertor is measured with wide-area divertor filter-scopes for each of the lines listed. Ion saturation current is measured with Langmuir probes, and only those probes calculated to be in the near-SOL of the outer-divertor is reported ($1.00<\Psi_N<1.005$). One can account for variances in exhaust power by normalizing the emission signals with P_{LCFS}, shown in the bottom panel. This quantity is calculated as follows:

$$P_{LCFS} = P_{\Omega} + P_{NBI} - \frac{\mathrm{d}W}{\mathrm{d}t} \tag{1}$$

where P_{Ω} is the ohmic heating power, P_{NBI} is the input neutral beam power and W is the stored energy of the discharge. For comparison, a mean heat flux calculated with Langmuir probes, q_{LP},

$$q_{LP} = \gamma \Gamma^{+}_{SAT} T_e \tag{2}$$

can be calculated using:

where γ is the sheath heat transmission coefficient (here assumed to be 7.5), J_{SAT} is the saturation current density and T_e is the derived electron temperature from the probe I-V characteristic. One can see that the heat flux derived with the Langmuir probes is roughly proportional to the power entering the SOL. A further point indicated by the same proportionality with saturation current is that the electron temperature derived by the Langmuir probes using the classical interpretation[11] is nearly constant over this range of input powers also indicating that only subtle changes are occurring in the vicinity of the strike-point. One can see in the third panel that the relative emission is unaltered by the strike-point location suggesting that the substrate material (i.e. graphite or LLD) makes no difference in the relative

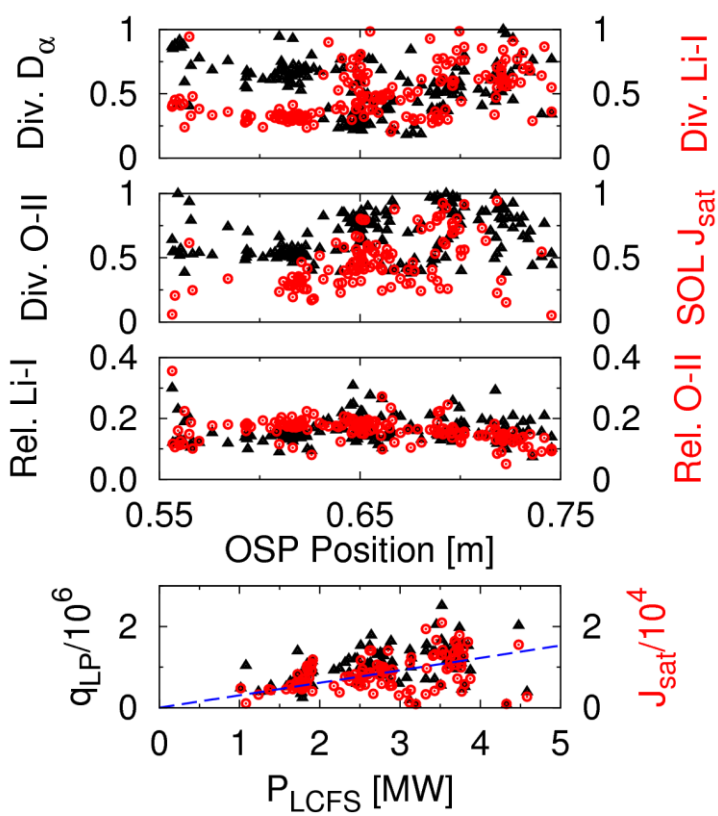

Figure 5.5: Relative emission of hydrogen (D-alpha) and impurities (Li and O) from the divertor of NSTX during LLD experiments. The LLD inboard edge is located at 0.65m. Incident particle flux is proportaionl to exhaust power (bottom panel) and can be used to normalize the emission data. Strong variation between graphite (ROSP<0.65m) and the LLD is not observed [10].

quantity of lithium or oxygen emitting in the divertor of NSTX during these experiments. This is consistent with the shallow-interaction depths expected from TRIM modeling and the rapid oxidation of lithium with the typical NSTX base pressure and leak rate.

Further evidence for the shallow interaction ranges determining the plasma performance is obtained from examining the overall discharge performance for the plasmas operated in FY2010. This is shown in Fig. 5.6 that collects data from the LLD experiments conducted throughout the entire run-year. As can be seen, a total of about 900g of lithium was deposited onto the PFCs in the machine, yet discharges from the beginning of the year showed similar performance as those at the end of the year with H97L~2 throughout[10]. As mentioned above, no dedicated experiment varying deposition *rate* was performed in FY2010 but is motivated by the contrasting performance noted above.

These two apparently contrasting data sets from FY2008 and FY2010 point to not only the need to explore the role of deposition rate, but also the underlying chemical state (i.e. any role of boronization) in determining the impact of lithium wall conditioning on overall plasma performance. Improved divertor diagnostics, such as more extensive Langmuir probe coverage, the MAPP system and improved coverage of the in-vessel PFCs by spectroscopic instruments will provide the base set of measurements to complement standard core diagnostics such as MPTS as well as magnetics. A key operational tool to aid in these experiments will be a new, upward-facing evaporator system, to be deployed in the first two years of

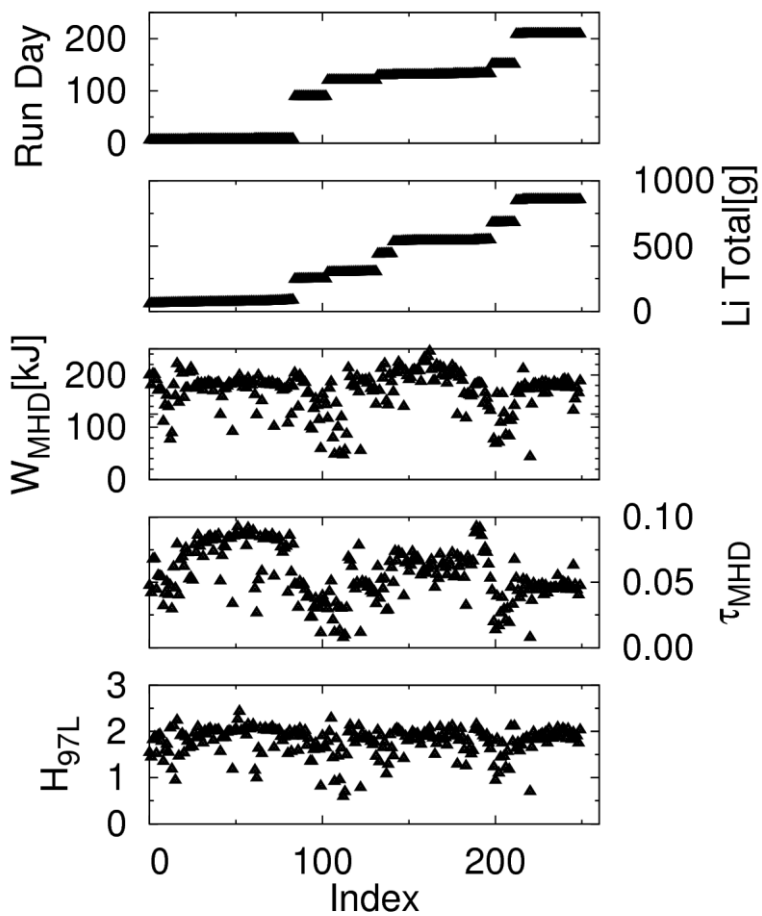

Figure 5.6: Selected entries from the LLD experimental database. Data indicates that normalized confinement was largely independent of the total quantity of lithium deposited in the machine[10] (though no systematic study of deposition rate was conducted). Dishcarges in this data set had input powers that varied from 2-4MW NBI, though yielded similar H-factors.

NSTX-U operations. As will be shown in section 5.2.2, significant fluxes of neutral hydrogen are expected on first-wall elements whereas LITER and LLD experiments focused on application of lithium to the lower divertor. Experiments in diffusive evaporation as well as with upward-facing evaporation system will enable studies on the effect of increasing the areal coverage by lithium. This is important to keep in mind when comparing boronization with lithiumization due to the fact that NSTX is traditionally boronized using a diffuse glow discharge that would cover nearly 100% of the PFCs whereas evaporated lithium with the existing LITER set is focused on the lower divertor alone.

The achievement of particle control with the use of lithium coatings has long been a goal for the NSTX program. The most recent data indicate that the surfaces are complex and evolving throughout the run campaign. While exploration of very low recycling ($R<0.5$) conditions remains a goal, it may not be possible to perform these experiments without more aggressive control of the lithium surfaces in the machine (existing analysis indicates PFC recycling has been reduced to about 0.9 in the NSTX, see chapter 4). This can be achieved with a fully flowing system and/or better vacuum conditions in addition to more complete removal of carbon contaminants. Therefore, in the first few years of NSTX-U operation, the transition toward including these elements will be studied as NSTX-U progresses to a state where another experimental campaign addressing the low-recycling state can be attempted.

5.2.1.1 Research Plans by Year for Thrust MP-1

Year 1 (2014) of the 5-year plan is ongoing before any NSTX-U tokamak experiments can be conducted. During this time, diagnostic check-outs will be conducted to ensure that key systems are ready at the start of discharges in year 2. Exposures of high-Z substrates on the LTX will be conducted with subsequent analysis. This will provide information to dedicated laboratory experiments both at PPPL and offsite on the interactions of lithium coatings on high-Z substrates in the presence of tokamak-relevant vacuum conditions.

- Additional analysis of NSTX discharges with the aid of interpretative and fluid models (e.g. similar to results shown in figure 5.9) will be conducted to identify key locations for QCMs, witness plates and marker tiles for use in NSTX-U. In the context of thrust 1, expected particle fluxes onto the MAPP diagnostic will be modeled for comparisons of experiments conducted in the following years.

- In the on-site surface science laboratories, the oxidation of thin Li films on single crystal Mo substrates, and compare to our previous measurements on TZM surfaces to elucidate the effects of grain boundaries and other non-uniformities in the oxidation of tokamak relevant

materials. We will expose Li-coated Mo with deuterium atoms and ions from a new ECR plasma ion/atom/hybrid source and measure D_2, D^0, D^+ uptake using temperature programmed desorption (TPD). Measurements before and after surface contamination with residual gases will illuminate the role of O in D uptake on solid and liquid lithium-coated substrates. We will study surface conditioning before initial loading with liquid metal to simulate recovery from surface oxidation, resolidification and maintenance vents.

- NSTX-U researchers will investigate surface wetting of Li films on Mo, TZM, stainless steel, and carbon films vs. temperature and oxide contamination using scanning Auger microscopy. Materials characterizations and UHV experiments will be performed to support the interpretation of results from MAPP and Magnum-PSI.

Year 2 - NSTX-U operation is expected to begin with all graphite PFCs with lithium evaporation and boronization. A boronization campaign will provide a baseline operating scenario from which to compare additional PFC and conditioning techniques. The MAPP diagnostic is expected to be available as well as QCMs, witness plates, target Langmuir probes, and standard spectroscopic diagnostics of the divertor plasmas.

- MAPP will be used to identify the basic state of the PFCs before the addition of lithium. For instance, MAPP can be used to measure the uptake of hydrogen due to both deuterium ions and neutrals derived from interpretative modeling creating an important validation for modeling efforts.
- Diffusive evaporation will be used to increase the areal coverage of the NSTX PFCs (in the event of incremental funding and subject to availability, an upward evaporation system will be used as well). With this capability, an injection amount identical to that used in the 2008 lithium introduction can be performed, except utilizing upper and lower coatings. This will identify the effect of increased lithium coverage on discharge performance as measured by thermal energy confinement time, impurity production and accumulation (via Z_{eff} of the plasma) and control of edge pressures.
- An important data set will be obtained by creating medium-to-low triangularity discharges that place the outboard divertor on the future location of the high-Z PFCs.

Year 3 - The introduction of high-Z PFCs will provide the opportunity to examine how this modest addition affects overall discharge performance.

- Comparisons of discharge performance with standard high-triangularity discharges vs. those diverting directly onto the PFCs will be made.
- Variances in deuterium uptake of lithium coatings on graphite vs. high-Z substrates identified in LTX exposures and offline experiments will be examined in the tokamak context. This will establish whether significant departures in lithium coating behavior are to be expected as an increasing amount of the NSTX-U PFCs are converted to high-Z. We expect to begin operations with no boronization and transition directly to lithium evaporations to perform the

specific experiment looking for any synergistic effect that may exist between boron and lithium.

Years 4 and 5 - NSTX-U will provide a comparison of particle control via lithium coatings vs. control with boronized walls and a cryo-pump. We expect to have at least an empirical understanding of deuterium uptake by lithium coatings and the associated changes in neutrals throughout the machine.

- Models of the surface uptake of hydrogenic species will be compared with hydrogenic control with the cryo-pump.
- In addition, examination of lithium coating performance at elevated temperatures will be examined with the heated cryo-plenum. This will inform on the impact of high-temperature lithium PFCs not directly under the divertor, but producing a flux impinging the SOL itself.

Throughout the 5-year plan, while MAPP provides in-situ measurements, simultaneous work in surface-science laboratories will make detailed measurements for comparison. These are also expected to focus on lithium-coatings on high-Z, metal substrates such as TZM-type molybdenum. The uptake of hydrogenic species and the impact of varying levels of impurities (e.g. C, O) on that uptake will be examined in the Li-metal system. This will provide information on whether such coatings can be expected to provide an absorbing surface once NSTX-U PFCs are upgraded to high-Z.

Years 3-5 will continue these initial studies of uptake and the impact on plasma performance an increasing amount of the NSTX-U PFCs are converted to high-Z. As the PMI processes create a mixed material on the PFC surface, this will likely impact the uptake of hydrogen and possibly impact machine performance. A combination of in-situ (i.e. MAPP) and ex-situ surface-science tools will be brought to bear to understand the basic physical processes occurring as the PFC surface is bombarded with plasma. A useful experiment will be to repeat the introduction of lithium performed in year 2 (i.e. begin operation without any low-Z coating). This would provide a measure of high-Z influx into the core plasma as a result of the staged implementation. In addition to studies of deuterium uptake, wetting studies on molybdenum and tungsten substrates of lithium, tin and gallium will be conducted in controlled laboratory settings to inform on the choice of liquid metal PFC for NSTX-U and conceptual design activities for the FNSF.

5.2.1.2 Baseline Deliverables for Thrust MP-1

1. Experimental determination of the role of areal coverage and boron+lithium chemistry on global discharge performance (e.g. energy confinement time)
2. Experimental comparison of lithium wall-pumped discharges vs. cryo-pumped discharges to examine the role large-area changes in PFC chemistry vs. localed pumping in the NSTX-U divertor. This includes the examination of deuterium uptake on clean and oxidized lithium-coated high-Z substrates over a range of temperatures.
3. Detailed characterization of PFC evolution during tokamak operations using the MAPP diagnostic system and coordinated laboratory studies.
4. Wetting studies of candidate liquid metal (lithium, tin and gallium) to examine the role of substrate and liquid impurities on wetting and film-rupture (i.e. exposure of the substrate).

5.2.1.3 Incremental Funding Research Plans and Deliverables

Increased resources will permit a more aggressive upgrade of the NSTX-U PFCs to a high-Z surface to eliminate the effects of lithium intercalation into the substrate material (see section 5.2.2.1 for more on lithium conditioning lifetimes and the impact of intercalation). This will also permit study of lithium coatings on a more reactor-relevant, metallic substrate. A closer integration of surface-science laboratories and tokamak sample exposures would be accomplished (e.g. improved surface preparation techniques to mimic in-vessel components and/or improved sample transfer capabilities).

5.2.2 Thrust MP-2: Unravel the physics of tokamak-induced material migration and evolution

Erosive fluxes are expected on first-wall components, thus limiting their lifetime, and the high power densities achievable on NSTX-U make it particularly well suited to examining issues of wall erosion. The edge plasma of fusion devices continuously interacts with a neutral population at the edge [5]. This creates a charge-exchange flux of high-energy neutrals that will impinge and sputter the first-wall. Recent papers have pointed out that wall erosion could result in thousands of kilograms per year of circulating material in a power reactor [19]. The eventual fate of the eroded wall material is unknown at this point and requires further study. This material has been conjectured to redeposit in the divertor region, where decades of effort have focused on creating a cool, non-eroding plasma [19]. NSTX-U research to be carried out to better understand material erosion is summarized in the following thrust:

Thrust MP-2: *A combination of quartz-crystal microbalances (QCMs), witness samples and marker-tiles will be utilized to provide measurements of shot-to-shot erosion and redeposition in NSTX-U. An upgraded MAPP system with QCM will enable shot-to-shot analysis of not just the quantity of deposited material, but also the composition of that material. The scaling of wall-erosion for typical NSTX-U divertor conditions over a range of P/S values will be used to construct a data-base to estimate/project total wall erosion expected for an FNSF or DEMO. The material transport variations as a function of divertor configuration (e.g. snowflake, detached, vapor-shielded) will also be measured and compared to simulation.*

In this section the erosive flux is estimated for an FNSF scenario based on the ST-pilot plant [5] to illustrate the magnitude of the material migration problem that must be solved. The proposed tools for measuring these processes are quartz-microbalances (QMBs), marker tiles and witness plate systems. An NSTX discharge is analyzed using the OEDGE/DIVIMP code suite to demonstrate the type of modeling that can be validated with improved diagnostic coverage in the upgrade. Erosion in the divertor region region, however, remains important for NSTX-U and for any future liquid metal PFCs. Collaboration with the Dutch Institute for Fundamental Energy Research (DIFFER) on the Magnum-PSI experimental device will provide an early opportunity to examine low-Z coating erosion from carbon and high-Z substrates ahead of operations in NSTX-U. This work helps inform on the lifetime of a given wall-conditioning technique (related to thrust 1) as well as the ability of NSTX-U to examine high-erosion divertor configurations as will be described in thrust 3. Finally, the baseline research plan will be presented alongside the deliverables expected at the end of the 5-year plan.

The ST-pilot plant is a 2.2m major radius machine with an aspect ratio of 1.7. The machine is designed for engineering Q ~ 1. The total fusion alpha heating and auxiliary heating power is about 250MW, and the duty-factor of the machine is assumed to be 0.3 (i.e. ~10^7 s/yr). Using the same assumptions of charge-exchange power as Stangeby,[19] the total erosion of the first-wall components would result in 1800 kg/yr (cf. Stangeby's reactor scenario calculates 8000 kg/yr). While this results in ~0.4 mm/yr of erosion from all the walls (assuming it is uniformly distributed), the consequence of redeposition in the divertor area is severe. Using flux-expansion numbers from Ref. [19], the area ratio of the first wall to the divertor is ~ 50. This results in a growth rate of ~17 mm/yr (assuming uniform redeposition in the divertor). It is difficult to predict how such thick layers will alter the PMI in the divertor. Given that this effect is configuration independent, it is clear that serious challenges face the extrapolation of any solid-material PFCs to a reactor scenario.

In principle, a plasma-facing liquid surface returns to its equilibrium position after being disturbed by transient events, i.e. it is a self-healing material surface. Similarly, for surfaces undergoing net erosion or deposition, a ready solution is available by the supply or removal of additional liquid from the PFC surfaces[20].

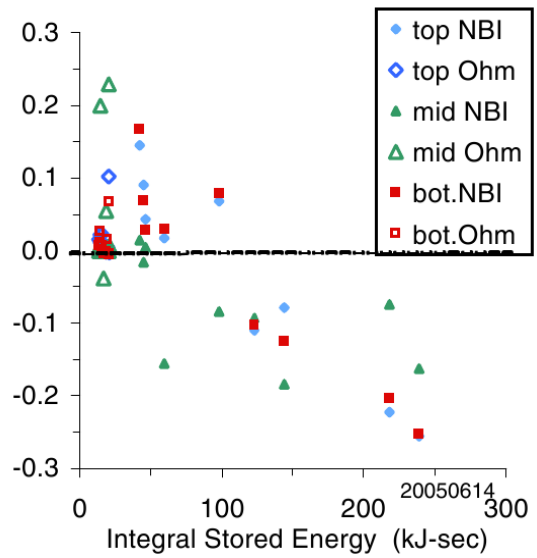

Figure 5.7: Change in mass (μg/cm^2) from 1 min. before a discharge to 1 min. before the next discharge plotted vs. the integral of stored energy and time. The legend denotes the location of the QMB (top, middle or bottom of the machine) and whether NBI or solely ohmic heating was used[21].

At full power, NSTX-U should provide about 15MW heating power to interact with approximately 30m^2, yielding a P/S ratio (in MW/m^2) ~ 0.5, whereas an FNSF pilot plant based on either an advanced tokamak or spherical torus would have a P/S ~ 1 [19]. Using estimates derived from [19], one could expect approximately 2.5nm of carbon to be eroded from first-wall components per NSTX-U discharge, i.e. within the measurement capabilities of QMB diagnostics with a sensitivity down to 0.7nm[21]. Erosion measurements have already been made in NSTX and are shown in Fig. 5.7 [21]. These indicate that the walls are already in a state of net erosion for NBI heated discharges (~5MW) that are sustained for about 1s (average stored energy is about 200kJ for these discharges). By providing multiple measurement locations with QMBs and other surface material diagnostics such as the MAPP system [22], we therefore expect NSTX-U to provide a suitable experimental platform for the study of wall erosion and the resultant deposited material. While carbon is expected to have limited utility as a reactor-relevant material, identifying material migration processes active in the tokamak edge will provide baseline information on the material transport processes assumed in [19], and how these estimates will impact a solid-wall option for FNSF. QMBs are not appropriate for use in high-heat flux regions of the machine, such as in the divertor. In these areas, marker tiles will be utilized to provide campaign-integrated measurements of the net erosion. Additional campaign-integrated measurements in the first-wall region will be made with witness-plate samples.

The equations used to generate estimates of first-wall erosion only provide order-of-magnitude estimates for an entire fusion device. If, however, erosion exhibits poloidal variation, then PFCs throughout the machine could be optimized to account for this and arrive at uniform component lifetimes. The type of analysis that can be carried out, and will be validated in the upgrade will now be demonstrated to provide an examination of just this type of poloidal non-uniformity.

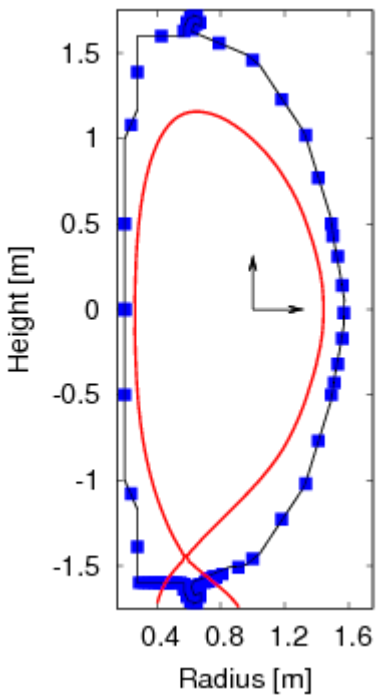

Figure 5.8: OEDGE model geometry for determining mean wall fluxes. Red outline shows separatrix location. Black lines indicate wall geometry. Blue points indicate sampling locations for obtaining an average wall flux measurement. Arrows indicate point of origin from which the poloidal angle (see fig. 5.9) is defined.

OEDGE/DIVIMP analysis is now possible in NSTX with the use of Langmuir probe measurements to reconstruct background plasma profiles[24] from which it is possible to model erosion of the plasma-facing components due to the combined effects of ionic and neutral bombardment. These models are constrained by measurements at the target plates and self-consistently solve the plasma-fluid equations including the hydrogenic neutral transport (see section VI: Theory and Modeling). The discharge modeled was conducted during the LLD campaign and had an 800kA discharge current with 4MW neutral beam heating. Two point modeling indicated a separatrix temperature of about 60eV. Divertor target density was found to be 3-5x10^{20}m^{-3} with a strike-point temperature of 3-5eV. Using OEDGE/DIVIMP, it is possible to extract the neutral particle fluxes throughout the machine as a function of location. Figure 5.8 shows the machine layout and Fig. 5.9 shows the corresponding neutral hydrogen flux and average energy at each location. The impinging neutrals originate from target recycling and charge-exchange processes at the plasma edge.

The mean energy on the outer wall elements ranges from 40-90eV which is already in the range where iron sputtering is expected (threshold energy of 44eV [27]) and at the threshold for molybdenum sputtering (threshold energy of 90eV [27]). As these are average incident energies there will be particles exceeding these mean values indicating that even in NSTX discharges, one could have expected molybdenum elements on the wall to be subjected to non-zero sputter yields. If one considers physical sputtering by the incident particles only (neglect chemical erosion), erosive yields of the outer first-wall elements are in the 1-5x10^{18} #/m^2/s range. This would result in mass loss of 0.002-0.01 ug/cm^2/s from ATJ graphite surfaces, equivalently 1.2-5.9 nm/s erosion rates. With a 5s discharge one would measure 6-30nm erosion – well above the detection limit of 0.7nm. This type of modeling and analysis can be validated in NSTX-U with the use of the expanded plasma and erosion diagnostic coverage.

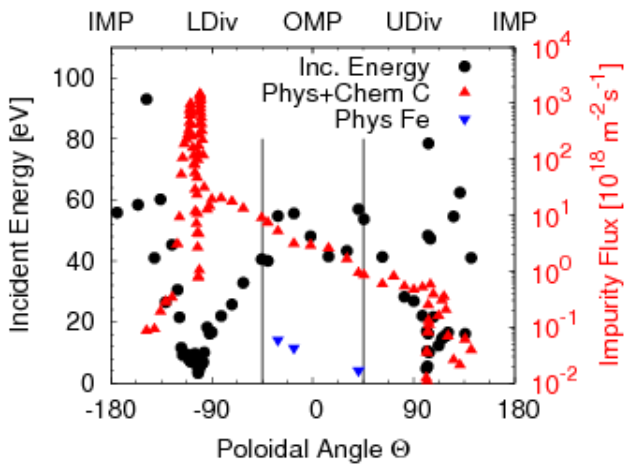

Figure 5.9: Neutral hydrogenic flux to wall elements derived by OEDGE interpretative modeling. Poloidal angle is defined from the plasma center indicated in figure 5.8. High flux at about -135 to -90 degrees is the lower inner and outer divertors. The out-board wall elements are found between 270 and 90 degrees and have incident energies of 40-90eV. Neutral flux to wall elements is the result of recycling and charge-exchange processes. Discharge simulated is 800kA, 4MW NBI heated discharge with a separatrix temperature of 60eV. Peak divertor density is 3-5x10^{20}m^{-3} with a temperature of about 5eV at the strike point (see ref. [24] for discharge parameters).

In the case of liquid metal walls, such transport processes will also occur. The key difference with liquids is the ability to replace lost material and remove excess quantities. The transport of material remains a critical issue for liquids, however, as any liquid metal PFC concept must demonstrate control of the liquid metal inventory to avoid in-vessel buildups. This transport of the liquid metal is particularly critical for the viability of lithium to any future device utilizing tritium. Due to the affinity of lithium to retain hydrogenic species, lithium that transports to remote locations in the machine will become a potential location for tritium retention inside the vacuum vessels.

Before examining whole-machine transport, it is important to assess absolute and net yields from the PFCs. This is typically done in ion-beam facilities [25] and linear plasma devices [26]. While plasma-devices are more relevant simulators than ion-beam facilities, the densities where these tests occur are often much lower than expected in a divertor (10^{18}-10^{19} vs. 10^{20}-10^{21} m^{-3}). In high-density divertor plasmas, ionization mean-free paths are expected to become comparable to the magnetic pre-sheath scale length and strong, local redeposition is expected. Simulations from Brooks, et al., indicated that redeposition fractions very close to 1.0 for tin or lithium can be expected in conventional divertor plasmas (30eV, 3x10^{20} m^{-3}) [29].

Newly-commissioned plasma devices are available to study this local material transport. The Magnum-PSI device is capable of producing high density, low temperature plasmas, similar to those expected in future power divertors [30]. Figure 5.10 shows a fast-camera image taken on the Magnum-PSI experimental device during experiments with lithium coatings. Figure 5.11 below is a quasi-2D simulation of lithium emission calculated using ADAS emission coefficients and experimental plasma profiles obtained on Magnum-PSI. Synthetic diagnostics based on these simulations show qualitative agreement in emission profiles and should be useful for validating local transport models for lithium, hydrogen and other impurities. Quantitative comparison indicates, however, that transport models based on ionization alone are not sufficient to reproduce the observed emission profiles. This makes Magnum-PSI experiments a unique testbed for examining recombination and charge-exchange effects in the expected low-temperature, high-density plasmas of future tokamak reactors.

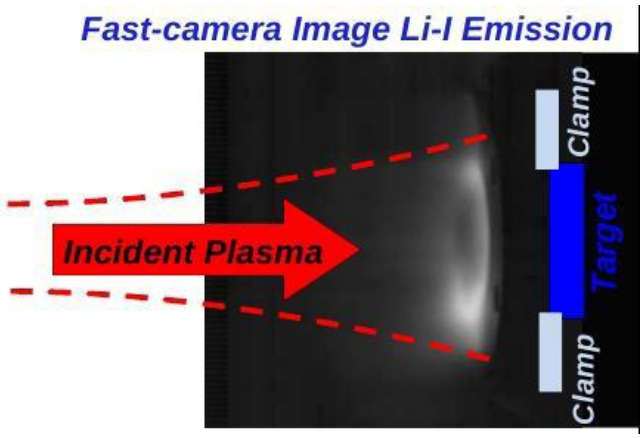

Figure 5.10: Fast camera image of Li-I (671nm) during experiments in the Magnum-PSI experimental device. Clamp and target designations are offset of the actual locations in the image for clarity.

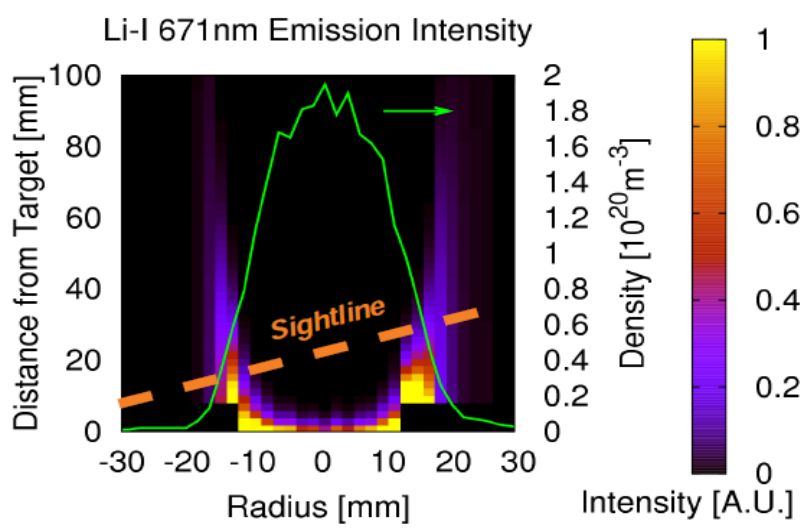

Figure 5.11: Simulated emission of Li-I (671nm) using quasi-2D transport models and experimental density and temperature profiles in Magnum-PSI. Synthetic diagnostics indicate a double-peaked emission structure qualitatively similar to the observed emission shown in figure 5.10.

Table 5.2 provides a comparison of various operational and plasma parameters comparing Magnum-PSI with NSTX discharges during heavy lithium conditioning with plasmas incident on the liquid lithium divertor [23, 24]. The comparison indicates that plasma produced in Magnum-PSI provide similar densities and temperatures as found immediately adjacent to the divertor target plates. The similarity in plasmas near the target indicates that studies of local material transport, and the interpretation of diagnostic signals in these dense divertor plasmas, will be able to inform on experiments in NSTX-U.

Table 5.2: Comparison of Magnum-PSI operational and plasma parameters with those found in NSTX (expected with NSTX-U). Plasma electron temperature, density and parallel particle flux are similar between the two machines as is the expected neutral pressure (≈1–3 [Pa]). The Magnum-PSI device targets can also be tilted with respect to the incident magnetic field to reproduce grazing incidence magnetic field effects near the target.

Parameter	Magnum-PSI	NSTX discharges with heavy lithium (Liquid Lithium Divertor)
Power	60[kW]	4[MW] NBI (15[MW] NSTX-U)
Pressure (source)[kPa]	10	N/A
Pressure target[Pa]	< 3	0.1–1†
T_e target[eV]	0.1–10	1–15
N_e target[m^{-3}]	10^{20}–10^{21}	5×10^{20} at strike point
T_i target[eV]	0.1–10	Unknown
Ion flux target [m^{-2}s^{-1}]	10^{24}–10^{25} (Normal inc.)	2×10^{23} at strike-point (≈ 3–5°)
Power flux [MWm^{-2}]	10	2–5 (≈ 3–5°)
Magnetic Field[B]	1.9 max.	0.6 (1 NSTX-U)
Beam diameter[cm]	10–15	≈4 FWHM med. triangularity
Pulse length[s]	12–110	1 (5–10 NSTX-U)
Bias [V]	$-100 < V_{target} < 0$	$-20 < V_{floating} < 20$

† Calculated using OEDGE interpretative modeling.

Experiments have already been conducted on Magnum-PSI and are undergoing analysis (shown in fig. 5.11). A lithium evaporator was used to deposit lithium onto sample of ATJ graphite, molybdenum (TZM alloy) and pure tungsten. In one experimental run, 100nm (50mg/m^2) of lithium was deposited onto the TZM sample and subsequently exposed to repeated, 5s discharges in Magnum-PSI. The central discharge temperature and density were varied for the experiments over a range of 0.7-2.7x10^{20} m^{-3} and 0.55-1.6 eV with the target biased 20V to simulate a typical bombardment energy expected in the NSTX divertor. By the end of eight 5s discharges (i. e., 40s of total plasma bombardment), lithium was still observed at the center of the samples. TRIM estimates of the sputter yield for a 20eV ion indicate a total yield of 0.0048, only 1/3 of which is sputtered as a neutral.[25]. A gross accumulated erosion over the 40s of bombardment can be estimated at 520mg/m^2, whereas only 50mg/m^2 were deposited.

One method of generating an estimate on the net erosion is to assume that if an additional (ninth) discharge had been performed, no lithium would have been observed. In other words, let us assume that by the end of the 40s all the lithium had been eroded, i. e., a worst-case estimate of the net erosion. In this case, a redeposition fraction for lithium on TZM, obtained from the relation N = (1-R)*G where N is the net erosion, G is the gross and R is the redeposition, is found to be ~0.9, integrated over a number of discharges with densities similar to those found in the NSTX divertor. Such long coating lifetimes on TZM indicate that lithium conditioning in the divertor of NSTX-U with a high-Z substrate could conceivably remain protected by the low-Z coating for a full 5-10s discharge despite large amounts of gross erosion.

Local redeposition has a profound effect on the amount of time a thin coating will remain in one location of the discharge due to the mitigation of the gross erosion rate. Lithium is known to have an increasing sputter yield above the melt temperature as well as a significant fraction of sputtering as ions [26, 28]. With the reported yields in references [26] and [28], estimates for the total yield of lithium neutrals due to evaporation and sputtering as a function of surface temperature. Figure 5.12 provides this estimate of neutral lithium yield for a given surface temperature with an incident deuterium ion flux from a plasma with density $5x10^{20}m^{-3}$ and temperature of 3eV with magnetic field lines incident at 3 degrees w.r.t. the plane of the target(parameters consistent with LLD divertor plasma conditions [24]). Based on these erosion yields the lifetime of a coating can be estimated as follows:

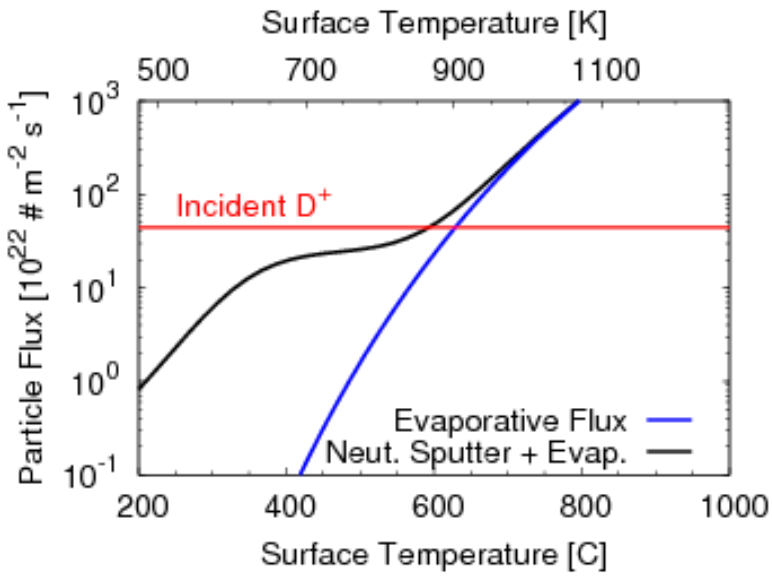

Figure 5.12: Particle fluxes as a function of surface temperature. The neutral lithium particle yield(black) is shown as a function of temperature when exposed to a plasma with density $5x10^{20}m^{-3}$ and temperature of 3eV at 3 degrees angle of incidence. 60% sputtering as ions assumed and removed from the yield curve[25]. Temperature enhanced sputter yield of the lithium is consistent with results reported in [26] and [28], though those studies consisted of low-flux plasmas or ion beams and extended to an upper temperature of 420 and 500C for [26] and [28] respectively. Two transitions can be observed in the figure: one beginning just above the lithium melt temperature that exhibits the temperature-enhanced sputter yield and the second occurring above 550C where evaporative flux begins dominating the total yield.

$$\tau = \frac{J_0 - J_{min}}{\Gamma_{gross}(1 - R_{redep})} \quad (3)$$

where J_0 and J_{min} are an initial and minimum areal number density of atoms, G_{gross} is the gross erosion rate and R_{redep} is the redeposition fraction.

Figure 5.13 shows the expected lifetime of a lithium coating as a function of surface temperature for conditions shown in Figure 5.12. Boron is not reported as having any temperature dependence of sputter yield and the estimated lifetime of an equivalent number-density coating under similar plasma conditions are 2, 22 and 220s for redeposition fractions of 0, 0.9, and 0.99 respectively. In any case should the redeposition fraction actually reach unity as calculated in [29], the coating lifetime tends to infinity. The existence of additional mass-loss terms, such as diffusion of the coating into the substrate material (as is the case with lithium on carbon) will reduce the coating lifetime.

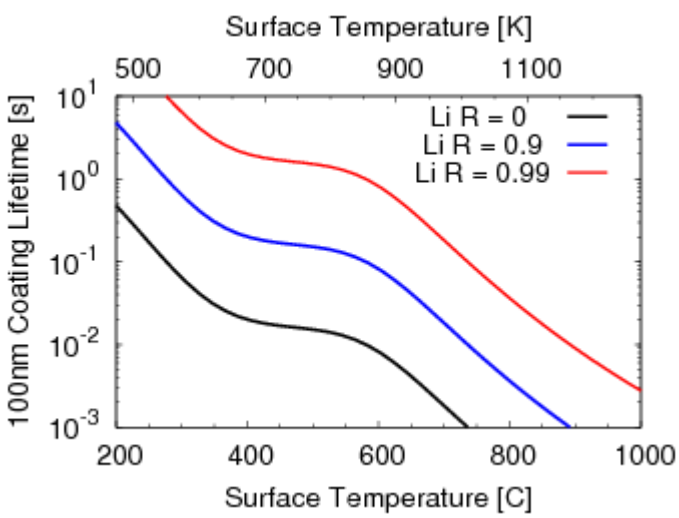

Figure 5.13: Lifetime of a lithium coating on a high-Z (i.e. non-intercalating) substrate for a range of surface temperatures and different assumed values of re-deposition fraction, R. The initial coating thickness is equivalent to 100nm (~50 mg/m^2) and is roughly equivalent to a typical NSTX lithium deposition of 100mg into the vessel. The minimum thickness for this calculation is taken to be 10nm (5mg/m^2).

Once initial studies of lithium depositions on carbon and molybdenum substrates have been carried out on Magnum-PSI, comparisons with results on NSTX-U will be conducted. Again, improved diagnostic coverage is expected in the form of improved Langmuir probe coverage of the upper and lower divertors, as well as more extensive spectroscopic coverage of the in-vessel components to aid in interpretation of local transport of material at the strike-points. More extensive QDM coverage, as well as the MAPP system will enable measurements of global transport. QDMs are not appropriate for use in high-heat flux areas such as the divertor plasma itself. In these locations, marker tiles will be fabricated and used to provide campaign-integrated measurements of thickness changes. Material transport codes such as DIVIMP [19] can then be used to begin linking local and global transport throughout the machine making use of plasma reconstructions based on measured plasma parameters.

With a staged implementation of PFCs, the material migration studies can be conducted with boronized carbon, lithiated carbon, bare high-Z substrate materials (e.g. TZM) and lithiated high-Z substrate materials. With the MAPP XPS capability, the composition of deposited films will be identifiable, potentially, on a shot-by-shot basis. With improved QDM coverage, first-wall erosion and redeposition can be characterized on a shot-by-shot basis. As the estimated first-wall erosion due to charge-exchange neutrals is closely tied with the machine P/S ratio, NSTX-U will be uniquely suited to study first-wall erosive fluxes (c.f. Table 5.1, ref. [19]).

5.2.2.1 Research Plans by Year for Thrust MP-2

Year 1 (2014) of this thrust presents strong overlap with the research plan in thrust 1.

- NSTX discharges will be modeled to determine optimal locations for key material erosion diagnostics such as the QCMs, witness plate samples and marker tiles. Expected fluxes to the MAPP location will be modeled in preparation for the following run years.
- While the above modeling and preparatory studies are occurring, additional experiments will be conducted on the Magnum-PSI device at FOM-DIFFER on lithium and boron coatings. In these experiments gross and net erosion (i.e. measurement of redeposition fraction) of high-temperature lithium PFCs will be measured for comparison to the estimates shown in figure 5.12.
- The effect of intercalation on coating lifetimes on graphite substrates will also be determined experimentally. In addition, the evolution of the film composition due to varying redeposition fractions will be studied to determine if in-situ cleaning by the plasma is a possible method of reducing film contamination (initial experiments already indicate reductions in oxygen content by 1-2s of plasma exposure in Magnum-PSI).
- Experiments at oblique incidence in Magnum-PSI will be conducted to validate models of redeposition at the relevant divertor magnetic configurations.

There is particular ITER relevance in the studies of mixed-material compositional evolution. At present, NSTX-U research create models of the lithium-oxygen-carbon system. A general approach to compositional evolution is being taken, however, such that provided sufficient atomic physics data, it should be possible to predict the evolution of beryllium-tungsten mixed materials under divertor or first-wall relevant plasmas in ITER.

Years 2 – This is the first full year of NSTX-U high-performance plasma operation and NSTX-U researchers will implement the full suite of standard divertor diagnostics such as target Langmuir probes and divertor spectroscopy as well as material migration diagnostics such as QCMs, witness plates and marker tiles.

- QCMs will be used to provide a shot-by-shot measure of mass gain/loss at the crystal location. Marker tiles will provide campaign-integrated measures of erosion/redeposition in locations where QCMs are not suitable (e.g. high-heat flux regions). Similar marker systems can be exposed with the MAPP system for shot-by-shot comparison of these complementary diagnostic systems.
- Using the standard divertor diagnostics, background plasma models will be constructed using any number of modeling tools (e.g. OEDGE, UEDGE, SOLPS are all run by NSTX team members at present).
- With this background plasma, material erosion and transport will also be modeled and compared to measurements (e.g. the fluid codes themselves have some capabilities to do this and additional tools can be brought to bear such as WBC-REDEP and DIVIMP as shown in figure 5.9). By the end of the second year a set of measurements of net erosion/deposition from various locations in the machine is expected to be available for comparison against the above codes. This would provide the base data set with all-carbon PFCs and lithium coatings.

An important question to assess with this system is the origin of carbon entering the NSTX-U core plasma. As indicated in the particle-control section of chapter 4, density rise is due, in large part, to carbon accumulation in the machine. However, recent analysis [60] indicates carbon yields are reduced by a factor of 3 in the divertor. What has not been clearly established is the relative importance of wall sources to the core impurity content. By measuring erosion from the first-wall components, a direct measure of the potential impurity source is measured. Combined with the aforementioned modeling capabilities, a clearer picture of the whole-machine impurity sources will be developed.

Years 2 and 3

- Wall erosion scalings will be established in the ST geometry as a function of input power, pulse length, edge neutral pressure. These scalings will determine the validity of estimates extrapolating wall erosion to long-pulse devices such as those given in section 5.2.2. Again, this topic has particular ITER relevance as NSTX-U will be conducting experiments to directly measure wall erosion due to charge-exchange and far-SOL particle fluxes. These will provide validation of plasma edge and impurity transport models such as OEDGE/DIVIMP.
- Coating lifetimes of boron and lithium that were examined and modeled in Magnum-PSI will

be measured in NSTX-U through the use of conventional plasma spectroscopy and marker tiles. This will provide validation of the material evolution models in the tokamak geometry. Coatings that erode and expose the high-Z substrate will provide the ability to measure discharge performance with the high-Z substrate in the near-SOL plasma as well as in the far-SOL.

- MAPP will be used to provide a means of measuring both total mass deposited (via the QCM) as well as the composition of the material (via XPS) to validate material mixing and transport models developed on Magnum-PSI.

Years 4-5 will concentrate on the impact of vapor-shielding on discharge performance and alterations in material migration. Of critical importance with the presence of lithium PFCs is the control of the invessel lithium inventory as it is expected to contain a significant amount of fusion fuels (in the case of a reactor, tritium). The question is particularly important to address in the vapor-shielded regime where large gross-erosion rates are expected near the strike-point due to a combination of sputtering and evaporation. Measurements of the changes in whole-machine mass deposition during experiments on vapor-shielded PFCs will be made to address this issue and identify locations where recollection of eroded and transported material would be ideal. In addition, the maximum temperature of first-wall elements with lithium coatings is another unknown. With the heated cryo-plenum, the impact of evaporating lithium into the SOL will be assessed (i.e. far from the strike-point region where redeposition is expected to be high). This will begin to determine the compatibility of high-temperature, lithiated, high-Z PFCs with good core performance.

5.2.2.2 Baseline Deliverables for Thrust MP-2

1. Characterization of gross erosion rates for high-temperature (>500C) lithium PFCs and redeposition fractions in typical divertor plasmas.
2. Characterization and modeling of net erosion/redeposition of the first-wall and divertor PFCs in the ST geometry.
3. Determination of the key parameters controlling erosive fluxes to the first-walls of the machine.

5.2.2.3 Incremental Funding Research Plans and Deliverables

In the case of incremental funding, we plan to increase the diagnostic coverage of first-wall elements to include more Langmuir probes and spectroscopic coverage as well as the possibility of neutral hydrogen sensors (both molecular and atomic). These diagnostics will provide improved examination of fluxes to and from the first-wall elements to provide a more complete picture of the processes controlling erosion at the edge.

5.2.3 Thrust MP-3: Establish the science of continuous vapor-shielding

Lithium has a significant evaporation rate at modest temperatures, such that early computational work on lithium PFCs indicated a temperature limit might exist at 350C[31]. Experiments at FTU, however, have demonstrated stable operation with a liquid lithium limiter up to 550C[32]. At these temperatures, a strong evaporation into the local plasma is observed simultaneously with reductions in limiter heat fluxes. This indicates a potentially attractive operating regime where strong local evaporation could lead to a continuously vapor-shielded PFC. Transient vapor shielding has been suspected to play a role in the prevention of PFC substrate damage during exposures to ELM-like transient discharges in the QSPA plasma gun [33]. An experimental determination of the ultimate temperature limits for a liquid lithium PFC in the diverted configuration as well as whether such a novel divertor configuration exists would help resolve these question. These considerations motivate the following research thrust:

> **Thrust MP-3:** *NSTX-U researchers will begin to establish the scientific basis and experimental demonstration of a continuously vapor-shielded surface in the tokamak environment with application to heat-flux mitigation. Extensive research on the long-pulse linear plasma device Magnum-PSI will be carried out to provide an extrapolable experimental demonstration of such vapor-shielding. These experiments will then be extended to NSTX-U using a lithium-coated high-Z substrate (for transient operation) or a flowing liquid lithium system (for long-pulse operation) with a high-power-density strike-point impinging on the PFC to raise the front-face temperature above the lithium evaporation temperature. MAPP, QCMs, Langmuir probes, and divertor spectroscopy, bolometry, and two-color IR diagnostics will be utilized to provide data for interpreting the results specifically examining the roles of lithium impurity radiation and vapor pressure-induced momentum loss on mitigating the incident heat flux.*

In this section, the expected temperature regimes of divertor PFCs in NSTX-U are shown to reach high temperatures – beyond those for which lithium erosion data exist at present (see thrust 2 above). For such high erosion rates, at least two possible methods exist to mitigate the PFC heat flux: plasma pressure reduction and plasma radiation, both of which will be described. The feasibility of examining vapor shielding in the baseline funding scenario (i.e. without flowing systems) will be discussed. As in previous sections, the baseline research plan will then be described followed by the deliverables expected from the 5-year plan.

As the generation of a lithium vapor shield depends on the generation of elevated substrate temperatures, it is necessary to estimate the temperature rise expected with the potential high-Z

substrate materials being considered for NSTX-U. If one assumes that the high-Z substrate is thick enough to make use of the semi-infinite solution, then the temperature inside the material as a function of position and time, T(x,t), is given as:

$$T(x,t) = T_{initial} + \frac{2q_0\sqrt{\alpha t/\pi}}{k}\exp\left(-\frac{x^2}{4\alpha t}\right) - \frac{q_0 x}{k}\mathrm{erfc}\left(\frac{x}{\sqrt{4\alpha t}}\right) \qquad (4)$$

where $T_{initial}$ is the initial temperature, q_0 is the incident heat flux, alpha is the thermal diffusivity and k is the thermal conductivity. The surface temperature exhibits a simple $t^{(1/2)}$ growth and is shown in Fig. 5.14 for a number of candidate materials, TZM-type molybdenum, tungsten and copper exposed to a 10MW/m^2 incident heat flux. The inclusion of copper is made in case an LLD-like substrate [18] should be used, i.e., a copper substrate with thin layers of stainless steel and molybdenum on top. In this case, the long-pulse thermal response of the PFC is dominated by the copper [34]. Without considering the metallurgical implications of these high temperatures (see section IV below), one can see that in all cases, the surface temperature of the PFC reaches as much as 800C in 5s under a 10MW/m^2 constant heat flux. As shown in Fig. 5.12 above, these temperatures are sufficient to equal and even exceed typical divertor main-ion particle fluxes observed in NSTX. Despite these high temperatures, with redeposition fractions greater than 0.9 Fig. 5.13 shows experiments can be conducted for reasonable lengths of time at elevated temperatures without resorting to extreme deposition quantities.

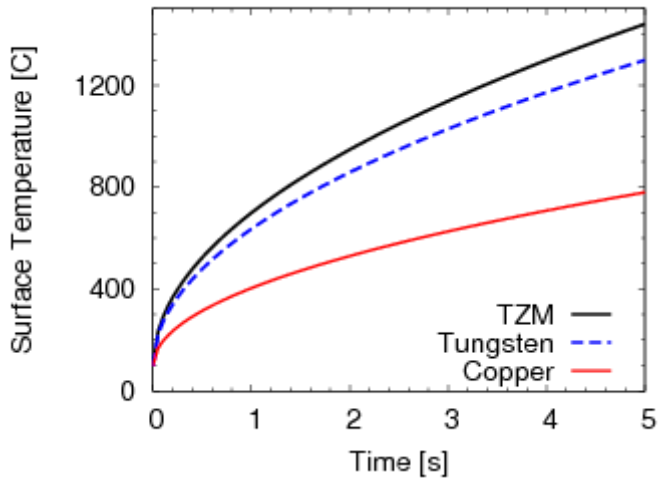

Figure 5.14: Surface temperature as a function of time for a constant 10 MW/m^2 heat flux for a number of candidate substrate materials, TZM-type molybdenum, tungsten and copper.

Given that elevated temperatures and coating lifetimes at these temperatures will be available in the NSTX-U, it is now necessary to consider what may set the ultimate lithium surface temperature in a tokamak divertor. One might consider a first limit on the surface temperature to arise from pressure-balance in a given scrape-off layer flux-tube. One way to estimate upstream pressure in the SOL as a function of input power is given in ref. [35] as:

$$P_{SOL} = 4\pi^2 R_0 a \kappa^{1/2} \frac{\chi_\perp}{\lambda_T} n_u T_u = 4\pi^2 R_0 a \kappa^{1/2} \frac{\chi_\perp}{\lambda_T} p_u \qquad (5)$$

where $p_u = n_u T_u$ is the upstream pressure, P_{SOL} is the power entering the scrape-off layer, R_0, a and κ are the machine major radius, minor radius and elongation respectively, χ_{perp} is the cross-field diffusivity at midplane and λ_T is the electron temperature gradient at the separatrix. χ_{perp} is typically estimated as approximately $2m^2/s$. λ_T can be related to the heat-flux width as $\lambda_T = 7/2\ \lambda_q$ in the limit that classical electron conduction dominates heat transport in the SOL. Using these typical values as well as the expected 3mm scrape-off layer width in NSTX-U as well as the machine geometry[3], one can create an estimate for the upstream pressure as a function of input power into the SOL. This is shown in Fig. 5.15. For comparison, Langmuir probe data taken during the FY2010 run campaign provides a measure of target pressure as a function of power entering the SOL. Also shown is the expected vapor pressure of a liquid lithium surface over a range of temperatures relevant to this study (500-1000C). As can be seen from the figure, very high temperatures of the lithium surface are required to approach the expected upstream pressures in NSTX-U high-power discharges.

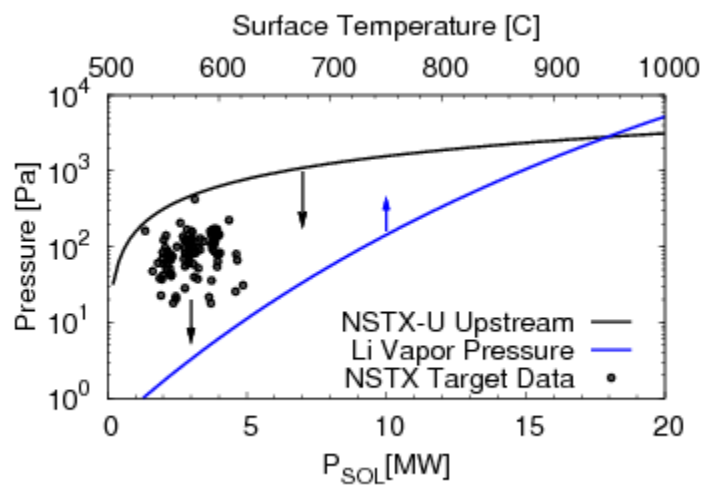

Figure 5.15: Comparison of pressures in considering vapor-shielded PFCs. NSTX-U upstream pressure estimate from equation 5 and NSTX divertor pressures as functions of power entering the SOL. The total lithium vapor pressure as a function of surface temperature is also shown for comparison. This figure indicates that even for NSTX discharges, lithium vapor pressure at surface temperatures of 750-800C would not exceed the divertor plasma pressure as measured by Langmuir probes at the target plate.

The figure informs on several aspects of the continuous vapor shielded regime. First, heat flux to the target due to the plasma charged particles as stated earlier can be rewritten:

$$q_t = \gamma \Gamma^+_{sat} T_e = \gamma n_{es} c_s T_e = \gamma c_s p_t; \quad p_t \propto \frac{P_{SOL}}{S_{plasma}} \qquad (6)$$

This shows that the heat flux impinging a target is directly proportional to the plasma pressure at the target. The total pressure in a given volume is the sum of all the partial pressures. In a strongly evaporating regime, then, the lithium vapor pressure may begin to significantly reduce the incident plasma pressure and provide a momentum sink.

Table 5.3: Comparison of non-equilibrium radiation powers of lithium in the traditional SOL radiation regime *vs.* a vapor-shielded plasma. Calculations assume 10% impurity fraction of lithium.

Case	$N_e[\mathrm{m}^{-3}]$	$T_e[\mathrm{eV}]$	$L_{char}[\mathrm{m}]$	$\tau[\mathrm{s}]$	$L_Z[\mathrm{Wm}^3]$	$P_{R,Z}[\mathrm{Wm}^{-3}\mathrm{s}^{-1}]$
SOL	5×10^{19}	50	15	4×10^{-4}	1×10^{-32}	2.5×10^{6}
Vapor-shield	5×10^{20}	3	1×10^{-3}	1×10^{-7}	1×10^{-31}	2.5×10^{9}

While the vapor pressure itself may provide a momentum loss term to reduce incident power on a target plate, lithium radiation is also expected to provide significant cooling. Figure 5.16 shows the estimated radiative loss function for lithium including transport effects (transport time tau). As can be seen in the figure, for short time-scales, lithium radiation can increase 5 orders of magnitude above the coronal equilibrium amount. Table 5.3 compares some transport time estimates comparing whole-SOL radiation to that expected in a vapor-shielded PFC. The key distinction is in scale lengths of a vapor-shielded PFC vs. the entire SOL flux-tube connection length. A vapor cloud of lithium is expected to extend scale-lengths of order the ionization mean-free path into the plasma. This is typically of order 1mm in a $10^{20}\mathrm{m}^{-3}$ target plasma [36]. The specific radiated power is calculated as:

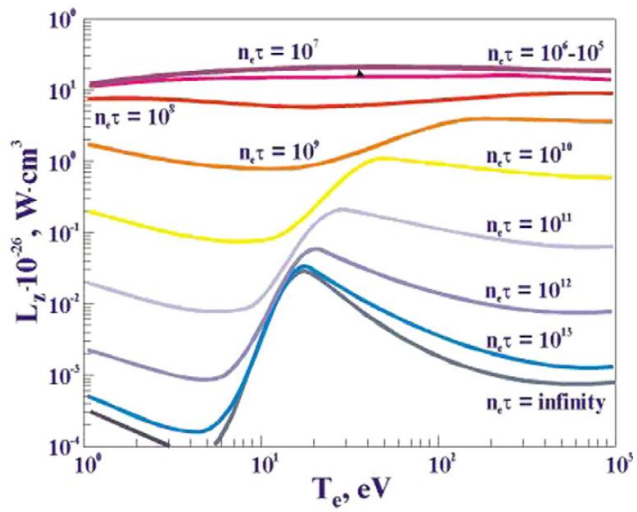

Figure 5.16: Radiative loss function (L_Z) for lithium in coronal ($n\tau$ = infinity) equilibrium and with transport effects included (finite $n\tau$) [37].

$$P_{r,z} = n_e n_z L_Z \tag{7}$$

where N_e is the electron density, N_z is the impurity density present in the plasma and L_z is the radiative loss function. This indicates the potential effectiveness of a dense plasma near the target to dissipate incident power in a novel divertor configuration. A key question regarding the results shown in figure 5.16 is how increased radiation is achieved at low electron temperatures (below 10eV). At low temperatures (below 10eV), radiation from singly ionized lithium will be difficult to achieve due to the very high ionization potential for the Li^{+2} state (75eV). Identification of power-loss mechanisms in low temperature plasmas (such as found in Magnum-PSI) and those found in the NSTX-U SOL will therefore provide insights into the radiative processes that will dissipate power in the lithium vapor cloud.

Although the radiative power is significant, several unknowns remain. The description used to evaluate the radiative power with the simple loss-function, L_z, is a simplification of the actual transport effects. Recent results have highlighted the importance of accounting for the strong density dependence found in lithium collisional-radiative models [38] and such considerations are not immediately apparent in results shown in ref. [37].

Modeling codes have been in development for a number of years describing vapor shielding in general for several years (e.g. [39]). Close experimental validation in a divertor-relevant plasma has not yet been accomplished. In addition, previous computational studies have focused on transient loading of PFCs. A primary aim of the present work will be to provide high-quality data from linear test-stand experiments as well as the tokamak itself in the steady-state vapor-shielded case to validate existing and new models.

In high-density divertor plasmas, ionization mean-free paths are expected to become comparable to the magnetic pre-sheath scale length and strong, local redeposition is expected. Simulations from Brooks, et al., indicated that redeposition fractions very close to 1 for tin or lithium can be expected in conventional divertor plasmas (30eV, $3x10^{20}$ m^{-3})[40]. This suggests that despite strong gross-erosion rates that might be expected in high-temperature lithium PFCs due to sputtering and evaporation processes, the net impurity ingress into the SOL will be substantially reduced by local redeposition. Such redeposition would also alleviate the amount of material a flowing system would have to source to the PFC surface. This allows initial studies even with limited inventories typical of LITER evaporations onto high-Z substrates relevant to examining the physics of high-temperature, vapor-producing PFC surfaces.

The production of substrate material into the plasma at the target plate ties this research thrust with the study of whole-machine transport described elsewhere in the five-year plan. In this particular topical area, however, more emphasis is placed on local transport near the PFC target, as this is where vapor shielding effects have previously been observed. It is therefore important to assess absolute and net yields from the PFCs. As multiple effects could be occurring simultaneously in a region that is difficult to diagnose, it will be important to obtain as much data as possible prior to attempting this divertor configuration on NSTX-U to ensure operational limits of the underlying substrates are not exceeded. Experiments conducted on linear plasma devices can provide this initial information. Experiments will be focused on demonstrating the concept of a vapor-shielded target, but also assess any impact on core-plasma performance. It is not unreasonable to expect that this divertor configuration could also alter the global transport of material throughout the machine. This would also be re-assessed, though with the benefit of the previous milestone on whole-machine transport in traditional divertor configurations.

5.2.3.1 Research Plans by Year for Thrust MP-3

Due to lithium intercalation into graphite, deposited layers quickly disappear, whereas layers deposited on molybdenum have demonstrate long life-times under similar plasma conditions. As intercalation is expected to occur at an even faster rate at elevated temperatures, experiments in NSTX-U on the vapor-shielded target will only be conducted after the high-Z, tile upgrade in year 3 of the 5-year plan. Before this, however, experiments will be conducted on the Magnum-PSI linear plasma device at FOM-DIFFER.

Years 1-2 (2014-2015)

- Experiments will be conducted on Magnum-PSI with a substrate temperature that varies from 300-800C during plasma bombardment. Both graphite and high-Z metal substrates will be tested and this plan is closely aligned with thrust 2. In these experiments, the local transport of lithium from the surface will be measured to determine the net erosion at the target which would help inform on available "pulse-length" under similar conditions in NSTX-U. These experiments will also provide important information on diagnostic methods and interpretations in this novel plasma regime (i.e. large spatial gradients, high-density, non-minority impurity fractions). Initial estimates of coating lifetime will be validated and refined before conducting experiments in NSTX-U on the high-Z PFCs. A key aspect of this work is the application of conventional diagnostic methods (such as filtered camera diagnostics and target Langmuir probes) to an unconventional divertor regime. This helps ensure that clear comparisons between conventional high-Z PFCs and vapor-shielded targets can be made.

Year 3 - high-Z tiles are expected to be installed into NSTX-U.

- The temperature response of these tiles to the NSTX-U heat fluxes without lithium and with lithium will be examined during this year. Namely, power density will be incrementally increased to validate the engineering design of these components, and develop operating scenarios that minimize the risk of damage under high-power densities.
- Initial demonstration of vapor shielding will be obtained by observing whether strong reductions in the incident heat flux are observed once the high-Z PFCs are coated with lithium. Specific measurements of plasma pressure will be made with divertor Langmuir probes. Surface temperature and heat flux will be measured with IR thermography. Thermocouples embedded in the PFCs will provide measures of integrated energy deposition. In the case of fast, eroding thermocouples, these diagnostics provide an additional measure of surface temperature.
- Divertor bolometry will be used to determine the total amount of radiated power from the near-target plasma. Traditional optical spectroscopy will indicate the amount of lithium and other impurities present in the plasma. If x-ray spectroscopy is available, then identification

of Li-II and Li-III emission will be possible (though Li-II is identifiable with 548nm emission). These diagnostics will all be applied to identify the existence of a vapor-shielding regime.

In years 4-5 we will begin to test the limits of vapor-shielding for reducing incident heat-flux and providing a protective buffer between the target and the plasma. These tests will focus on establishing the operating space of the vapor-shielded regime and compatibility with good core performance. In addition to experimental studies, expanded modeling is expected to occur to extend new and existing fluid models to this high-density, high-impurity fraction regime.

In the event that a full-funding scenario should be applied, we expect to be able to implement a fully-flowing liquid metal module for installation in the NSTX-U vacuum vessel, assuming laboratory testing indicates the technology is sufficiently advanced to do so. In this case, the liquid system would provide continuous replenishment to the surface and long-pulse testing of the vapor-shielded target could be conducted even with reduced redeposition rates. Initial tests with the device under plasma bombardment will also determine whether a flowing system is, in fact, able to maintain an equilibrium impurity concentration of the surface in contact with the plasma.

5.2.3.2 Baseline Deliverables for Thrust MP-3

1. Determination of existence of continuous vapor-shielding regime in the NSTX-U divertor.
2. Determine roles of pressure and radiation as means of reducing incident heat loads to the PFC surface.
3. Determine required flow rates and replenishment of liquid lithium for demonstration of continuous vapor-shielding for long-pulse.

5.2.3.3 Incremental Funding Research Plans and Deliverables

In the incremental funding scenario a fully flowing, liquid lithium divertor module is planned. With this module, it will be possible to extend the amount of time the target sustains vapor-shielding well beyond the pulse-length estimates shown in Figure 5.13. In this plan, then, long-pulse demonstration of the concept will be possible. In addition, efforts would be made to increase the diagnostics in the divertor, in particular, a spatially-resolved, spectrally-resolved instrument could provide key insight into the radiating species and could strongly constrain codes attempting to describe this new divertor regime.

5.3 Plasma-Facing Component Research & Development

In order to clearly identify the effects of changing the PFCs and base materials present within NSTX-U, it is planned for a staged upgrade over the next 5-years. Such a plan requires coordination over the entire 5-year plan and depends on the creation of a base set of diagnostics early in the plan as well as a set of reference discharge scenarios. By returning to the reference data sets, modifications to machine performance as a result of incremental changes to the wall and divertor PFCs will be examined in detail.

Figure 5.17 shows the upgrade scenario proposed for the base budget case. Operations begin in 2015 with carbon divertor and wall PFCs. As indicated in the research plans above, reference plasmas will be established in this first year and compared to subsequent years. The first of these modifications will be the introduction of a high-Z divertor target in 2016 (the technological choice for this PFC is discussed in the section below).

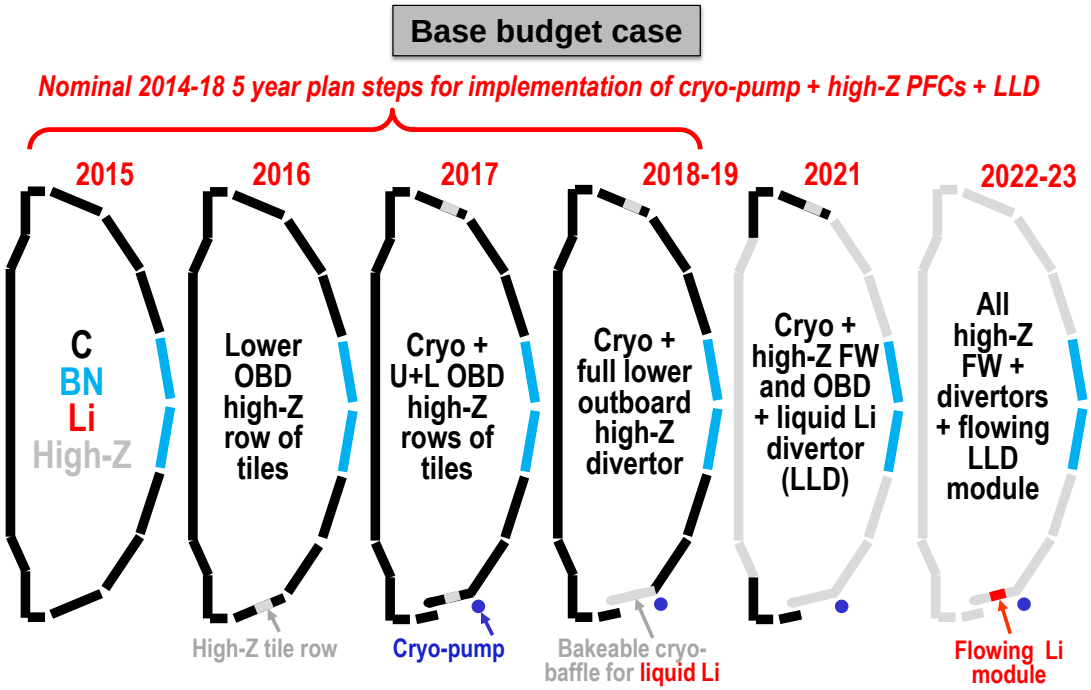

Figure 5.17: Implementation schedule for cryo-pump, high-Z plasma-facing components, and flowing liquid lithium divertor module with base budget funding.

As indicated above, this year will begin operations without a boronization campaign to establish the effect of the boron on the lithium-carbon chemistry (see thrust 1 description above). This also allows for erosion studies to be carried out on the bare high-Z tiles prior to lithium evaporations. This staging also allows a comparison between a high-Z divertor target and the

previous carbon target (in low triangularity discharges) before the divertor geometry is altered for the cryo-pump upgrade. The first immediate benefit to the Materials and PFCs research plan is to provide a non-intercalating substrate enabling high-temperature lithium to be studied with a lifetime limited only be erosion and redeposition as opposed to the additional effects of graphite intercalation.

The cryo-pump upgrade represents a substantial outage period and is planned for the 2016-2017 break. During this this, the high-Z target set that was previously installed on the lower divertor will be moved to the upper divertor while a similar row of high-Z targets is installed on the cryo-pump plenum. This upgrade allows low-triangularity, double-null discharges to divert on high-Z simultaneously. It will also allow impurity studies to be made comparing the effect of a high-Z source localized near the divertor (i.e. 2016 in lower-single null) and the addition of a high-Z source localized on the first-wall (i.e. 2017 in lower-single null).

In the 2018-2019 time period, a full, high-Z cryo-pump plenum is planned. This plenum will be heatable to support bake-out as well as experimental studies. This upgrade will provide data on the effect of increased high-Z divertor coverage and enable experiments on changing the pre-discharge PFC temperature. For example, it may be beneficial to operations to liquefy lithium coatings very soon after a discharge begins. By pre-heating the cryo-baffle to (say) 150C the temperature difference is reduced leading to a faster transition to nominally liquid lithium surface temperatures. Such a strategy was suggested by LLD experiments in the 2010 run campaign but could not be re-examined before the beginning of the upgrade.

In the second 5-year plan, a conversion of the first-wall components will be accomplished by 2021. By retaining graphite PFCs in the divertors but completely converting the walls of NSTX-U to high-Z, the complementary experiment to the LLD can be performed. That is, the LLD sought to address the question of how performance changes when $1m^2$ of the divertor is converted to a high-Z substrate with lithium coatings. By converting the walls, we can ask what effect changing the other ~90% of the PFCs will have on discharge performance. This strategy also maximizes the time available to complete scenario development including heat-flux mitigation schemes such as radiative divertors, snowflake configurations, vapor shielding or combinations of the above. By 2022-2023, the NSTX-U will be converted to a full, high-Z machine.

In addition to the high-Z PFC conversion, a fully-flowing liquid lithium module will be tested by 2022-2023. A number of technical challenges must be addressed before implementation of such a device in a tokamak and are described below. This device will enable long-pulse operation in the continuously vapor-shielded regime. It will also enable demonstration of Li-surface purity control by continuously replacing the surfaces that getter residual vacuum gases with fresh Li.

The baseline budget case can be accelerated in the event that incremental funding is made available as shown in Fig. 5.18. In this budget case FY2016 remains identical to the baseline budget scenario. The long outage to install the cryo-pump is utilized to upgrade the wall to high-Z PFCs. This effectively advances the NSTX-U PFC upgrade program 4 years. This funding would further impact the development and testing of a flowing liquid lithium divertor module to be installed early in the next 5-year plan followed by a full toroidal flowing lithium divertor in 2021.

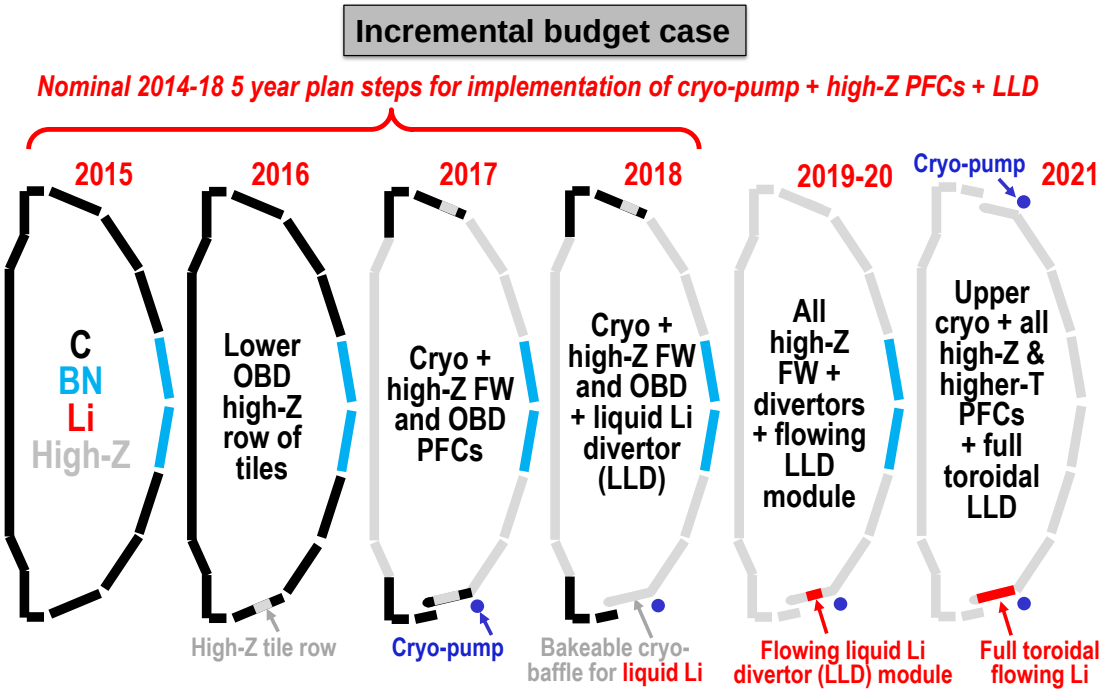

Figure 5.18: Implementation schedule for cryo-pump, high-Z plasma-facing components, and flowing liquid lithium divertor module if incremental budget is funded.

The remainder of this section describes the research program on PFC technology to support the NSTX-U PFC upgrade plan.

5.3.1 Staged Solid PFC Upgrades

Research on an appropriate high-Z target PFC will be conducted in the time leading up to the first outage. Tungsten and molybdenum are both considered candidate materials, though tungsten is preferred due to its relevance to FNSF and potentially, future reactors. Molybdenum is considered an option due to at least two attractive features: 1) a lower sputter threshold will create a larger "signal-to-noise" ratio for material migration studies, 2) molybdenum components are more easily fabricated than tungsten. (Of course, during operation, a higher erosive yield

may prove a liability if core contamination cannot be addressed, but this is a potential problem for any high-Z PFC in a confinement device.) Both materials are compatible over a wide temperature range with all liquid metals currently considered for fusion experiments: Li, Ga, Sn and alloy combinations of these metals.

Several technological options exist for deploying high-Z PFCs within a tokamak experiment. These include application of a thin, high-Z layer on a copper substrate – essentially duplicating the FY2010 Liquid Lithium Divertor module. The next option is to utilize a single high-Z bulk tile – another option developed for the NSTX divertor immediately prior to the upgrade outage (though never tested under plasma operation). A third option is to utilize thin-film coatings of the high-Z on top of existing graphite tiles which is identical to the approach taken by ASDEX-Upgrade [41]. Finally, high-Z structures can be constructed in a lamellae shape as done on C-Mod [42] and JET [43]. Physical processes related to the thermo-mechanical performance of each of these options have already lead to a preference for a lamellae structure in the divertor and thin-film coatings for first-wall PFCs. The following provides a brief description of these considerations.

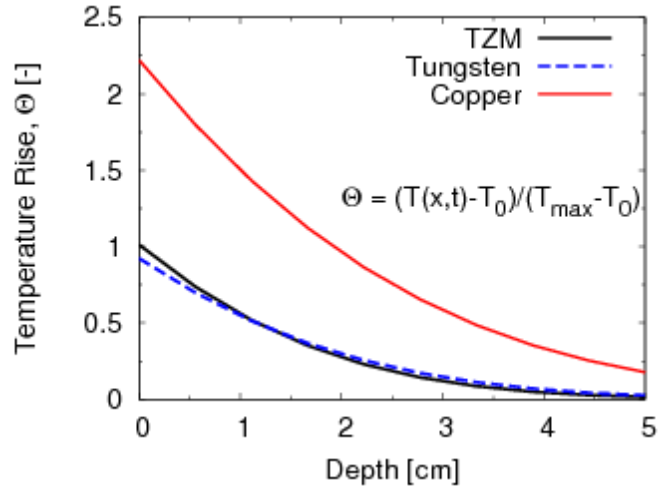

Figure 5.19: Non-dimensional temperature rise as a function of depth into a PFC material at 5s discharge time with 10MW/m^2 incident heat flux. Maximum temperature is defined as the recrystallization temperature of the metal ($T_{recryst}$ ~0.5 T_{melt}).

The first considerations are the temperature limits of the material from a metallurgical perspective. The internal temperature profile given in eq. 4 above is shown as a function of depth into the material at 5s of discharge time in Fig. 5.19. In this figure, the temperature rise is non-dimensionalized with the initial and maximum temperatures allowed by the material itself. This maximum temperature is taken as the recrystallization temperature of the material for which representative values are 1425, 1400 and 400 C for TZM-type molybdenum, pure tungsten and copper respectively. The initial temperature is set to 100C. As can be seen in the figure, both TZM and tungsten would be expected to reach the maximum temperature in 5s under constant heat flux whereas copper exceeds the allowed temperature rise by more than a factor of 2. This essentially eliminates the LLD-like construction from consideration for 5s pulses at 10MW/m^2 incident heat flux (though for lower heat flux regions, or reduced pulse lengths it may still be considered).

The next criterion will be the ability of the material to withstand thermo-mechanical stresses that arise due to large temperature variances between the surface and the back-face of the material. For example, the molybdenum tiles designed for NSTX FY11-12 run campaign could only withstand 2 MW/m^2 average surface heating for 1s before thermo-mechanical strains exceeded allowable margins. This is clearly unacceptable for NSTX-U and would need to be improved. In other machines using high-Z divertor targets such as CMOD[42] or JET[43], the bulk metal is fabricated into lamellae. By segmenting the bulk metal, thermal-mechanical stresses can be alleviated for a given depth of material. The material depth is determined by the desired thermal capacity of the PFC. For instance, in the case of TZM and W shown in figure 5.19, the implied depth of each lamella would be at least 5cm for the semi-infinite thermal solution to be a valid estimator.

It is also possible to create PFCs qualified for operation in the divertor with the use of high-Z coatings on graphite tiles as shown in the ASDEX-Upgrade device[41]. In this scheme the coefficient of thermal expansion must be closely matched between substrate graphite and the high-Z coating. Indeed, ASDEX-Upgrade made use of a specially formulated graphite for this purpose. This does not, however, completely eliminate stresses which can still arise in differentially-heated objects. The adhesion of the surface coating to the substrate is process dependent and several had to be investigated by the ASDEX group before the current design was settled upon. Even in this event, excessive heat fluxes can lead to failure of the coating and exposure of the underlying graphite. In regions of reduced heat flux, however, these thermo-mechanical considerations become less severe and it may be possible to use relatively simple coating technologies to convert the existing graphite tiles.

These last considerations lead to favoring a bulk-W, lamellae design for the divertor target and high-Z coatings of first-wall PFCs where surface heat-fluxes are less of a concern. Prior to implementation, further research on these two options will be conducted in the form of prototype fabrication and testing at suitable heat-flux facilities.

5.3.2 Liquid-Metal Plasma-Facing Component Research and Development

In years previous, the usage of liquid lithium for particle control has been emphasized based on the results observed on TFTR, CDX-U and NSTX with the reduction of lithium as well as the measurements of deuterium retention in PISCES-B. As discussed in section 5.2.1, the vacuum conditions as well as shot-timing used in NSTX (and expected in NSTX-U) create a complicated surface and introduce significant technical challenges to obtaining a “pure” lithium PFC surface

where the recycling coefficient might be expected to remain below 0.5. This motivates examination of a fully-flowing liquid PFC to reduce the residence time of the liquid in contact with the background vacuum conditions as well as a means of removing the gettered materials. In addition to this long-standing scientific goal of studying the low-recycling plasma regime, liquid metals generally offer several advantages over solids as discussed in the introduction. These include the elimination of permanent reshaping of substrate PFCs under plasma bombardment and separation of PMI problems from neutron irradiation problems. As indicated in Figure 13, the amount of time available for high-temperature PFC experiments will be paced by the redeposition fraction. Providing a flowing system to replace the lost material will enable extension of high-temperature regimes to long-pulse operation.

In order to examine these potential benefits in a tokamak device, significant development is required, but must be accomplished in the next 5-10 years if experimental data is to be available to inform on a liquid-metal option for an FNSF.

Progress in understanding liquid metal PFCs has already been accomplished with the Liquid Lithium Divertor in NSTX. Experiments with the NSTX LLD campaign has resulted in several important results related to the implementation of liquid metal PFCs[44]. First, the LLD confirmed the result on limiter machines that liquid lithium provides a protective layer over a high-Z metal substrate. Next, the LLD demonstrated a stable liquid metal using a porous substrate for the first time in a diverted tokamak. In addition to the liquid metal stability, the overall construction of a porous metal substrate was able to successfully operate the entire run year without evidence of damage during post-mortem analysis.

Proceeding from this work, internal development of a liquid metal loop facility is ongoing at PPPL for the demonstration of basic flow control and candidate LM PFCs in NSTX-relevant vacuum conditions. The laboratory tests will inform on whether the basic concept of using flow to control the gettered impurities is feasible. The facility will also demonstrate the basic operation of LM-PFCs so that a transition to NSTX-U will be made as smoothly as possible. Due to the inherent needs of LM-PFCs of the type being development, integral active cooling will be demonstrated in the offline facilities as well.

Alongside development of the loop facility, additional tests on Magnum-PSI will be carried out using pre-loaded liquid metal target samples. These will contain an integrated reservoir of liquid metal to examine issues related to porous-MHD and surface stability in the Magnum-PSI, magnetized plasma environment. They will also enable studies at very high temperatures (e.g. >600C) to explore the continuous vapor-shielding regime and how it extends to long-pulse operation.

In the incremental budget scenario, we plan to demonstrate sufficient technological progress to warrant a fully-flowing, liquid metal divertor module in NSTX-U by the FY2019 (2022 in the baseline scenario). This ambitious goal will provide an experimental divertor target to demonstrate the linkage between all three physics thrusts in this TSG. That is, surface contamination processes studied in the lithium surface-science will inform on the expected surface composition, uptake of deuterium and/or other impurities such as oxygen, and any impact these have on the resulting plasma interactions. The module will provide a temperature-controllable system for examining variations in whole-machine transport that might occur in a transition from low temperature liquid lithium PFCs to high-temperature surfaces. Finally, at high-temperature, long-pulse continuous vapor shielding phenomena could be studied with such a module. This cap-stone project would provide the technical basis for a whole-divertor upgrade to a flowing liquid metal PFC in the next 5-year plan for NSTX-U and strongly inform on the liquid metal option for FNSF.

5.4 Theory and Modeling

The theory and modeling required in support of the three research thrusts overlaps with that of the Boundary Physics TSG in that understanding plasma-material interactions (PMI) and their impact on the core plasma requires a characterization of the incident plasma, as well as an ability to predict the transport of the products of PMI. We will describe below the anticipated role of those codes in M&PTSG research, but refer the reader to the BPTSG chapter for more detailed descriptions.

The codes and models to be described here can be divided into three types:
Materials and atomic physics. These are first principles, or nearly so, descriptions of physics at the smallest relevant scales, femtometers to nanometers.
Surface chemistry and evolution. These codes combine analytic and theoretical descriptions of the material and its state with empirical models where a more fundamental understanding is lacking. This is a relatively new category of tokamak modeling.
Global transport and surface evolution. These codes attempt a comprehensive description of the tokamak environment, including both the material surface and the plasma.

5.4.1 Materials & Atomic Physics

5.4.1.1 Monte Carlo Plasma-Surface Interaction Simulations

Codes like TRIM [45] and comparable variants VF-TRIM (U-Illinois) and SRIM (www.srim.org) rely on the fact that for energies above a few eV, the interaction of an incident

ion or neutral can be described theoretically in terms of multiple binary collisions between the incident particle ("projectile") and atoms in the material surface ("target"). Given a comprehensive characterization of the chemical and structural composition of the material, a Monte Carlo procedure for simulating the resulting chain of collisions can be carried out. The end result of a statistical sampling of such calculations is a set of probabilities for absorption or backscattering of the particle and sputtering of target atoms. Distributions of the outgoing energy and velocity vectors for the backscattered and sputtered particles are also accumulated. All of these outputs are functions of the incident particle's energy and angle relative to the surface normal.

TRIM has long been, and continues to be, a "workhorse" code for simulating PMI because it can produce comprehensive and kinetic characterizations of these processes. The first and most obvious limitation is that it can be applied only to a known and constant material state. In contrast, material surfaces in operating tokamaks are steadily evolving and poorly characterized. A second related limitation is that in attempting to model realistic surfaces, adjustable parameters, such as the surface binding energy, must be estimated or guessed. Finally, the binary collision assumption is known to break down for incident energies of a few eV or less when the incident particle interacts with multiple target atoms.

5.4.1.2 Molecular Dynamics Codes

Such regimes are the realm of molecular dynamics codes. They attempt a closer to first principles characterization of the same problem. In a molecular dynamics (MD) code, the atoms of a three-dimensional portion of the surface are explicitly simulated, with their mutual interactions and the interactions with the incident particles described by a specified interatomic potential. In quantum MD, these potentials are computed "on the fly" by solving Schroedinger's Equation for the relevant electrons in the atoms. Because of the computationally intensive nature of MD codes, the time and space scales that can be simulated are extremely small (femtoseconds to picoseconds; length scales smaller than nanomoeters). Like the TRIM-type codes, one needs to know the surface composition of the material to simulate the PMI. The other principal limitation of MD codes is that accurate potentials are known only for a few, relatively simple systems.

The potential for using MD codes to obtain an improved understanding of the behavior of lithium in NSTX (and other devices) has been already demonstrated by Krstic et al. [46] (Sec. III-1), and we anticipate similar contributions in the future to the "Lithium Surface Science" thrust.

5.4.1.3 Atomic Data and Analysis Structure Database

The Atomic Data and Analysis Structure (ADAS) [47] is now the principle resource for atomic

physics data used (and supported by) the fusion community. ADAS is first a database of fundamental atomic physics cross sections contributed by physicists from around the world. ADAS is second a collection of numerical tools for massaging and assembling those data into a form useful by both fusion experimentalists and modelers. The particular quantities of interest for the M&PTSG (in all three thrusts) are effective rates for ionization, recombination, and line radiation emission of the relevant impurities (neutral and ionized), Li, O, B, C, etc. These "effective" rates are obtained by invoking the assumption (usually valid) that the electronic excited states of ions and atoms equilibrate amongst each other much more rapidly than they do with the ground electronic state. The resulting "collisional radiative" (CR) model allows for the (extremely important at high densities) effects of the excited states to be condensed into effective rates for the ground state species.

ADAS has CR rates for all of the atomic species of interest to the M&PTSG, although with varying degrees of accuracy. The bulk of the fundamental cross sections in the CR model must be computed by sophisticated, and expensive to run, atomic physics codes. As these practitioners work their way up the periodic table, better cross sections are obtained. Presently, such data (and CR models) are available for hydrogen and lithium; carbon, oxygen, and boron model rates rely on older data. The assumptions of the CR model itself are another source of uncertainty. Particularly in the "continuous vapor shielding" regime, these uncertainties may translate into large uncertainties in simulations replicating this operating regime [48]. For this reason, experimental and theoretical work is planned to validate aspects of the CR model for lithium.

5.4.1.4 Surface Chemistry and Evolution Modeling

Developing a truly predictive plasma transport capability will require comparably realistic models of particle and heat transport in the plasma facing materials. Heretofore, plasma transport codes (those in the next section) utilized characterizations of materials and plasma-material interactions, via TRIM or MD codes, that typically assumed pristine, idealized materials. In this Five Year Plan, NSTX-U modeling efforts will begin moving beyond these simplistic models toward ones that allow the material surface to evolve in response to plasma fluxes.

The two codes listed below are being considered for this purpose. However, concerns with usability or suitability for the NSTX-U application may lead to the development of new, but similar, tools.

5.4.1.4.1 WallPSI (UCSD)

The WallPSI code [49] solves transport equations for particles and heat in the material surfaces. As such, it provides a realistic characterization of all processes affecting the hydrogen content of

the surface, including recycling and retention. Impurity erosion processes, including physical sputtering, chemical sputtering, evaporation, and radiation enhanced sublimation are all included with physically realistic models.

WallPSI was developed as part of the FACETS project [50] and was designed to be coupled to plasma transport codes (namely, UEDGE), but it can also be run in a stand-alone mode. For example, [51] describes stand-alone applications to simulate PISCES materials experiments. Analogous applications of interest to NSTX-U could be made in simulating experiments on the Magnum PSI linear device or on smaller lab experiments being carried out in connection with the NSTX-U program.

5.4.1.4.2 WallDyn (IPP-Garching)

The WallDYN code [52] provides a consistent, global solution to the impurity erosion-redeposition problem for a given plasma condition. The principal input is a matrix of transport probabilities describing the likelihood that an impurity eroded from one particular location in the vessel will be transported to a second location. The elements of this matrix are computed with an impurity transport code, say, DIVIMP using that same plasma condition. The basic version of WallDYN uses relatively simple characterizations of the material surfaces, although the most recent version [53] allows the thickness of the surface layer to evolve in time and deposited species to diffuse into the material.

Considerable evidence exists for impurity migration occurring via many small erosion and redeposition steps. The global and consistent solution obtained with the matrix approach used by WallDYN captures this behavior in an effective and efficient way. Since material migration represents one of the three M&P thrusts, a tool like WallDYN would be useful in interpreting the corresponding NSTX-U experiments.

5.4.1.5 Global Transport and Evolution Simulations

Because these codes provide a characterization of the effects of changes in a plasma facing surface on the plasma conditions elsewhere, they will likely prove useful in all three M&P research thrusts.

5.4.1.5.1 SOLPS (IPP-Garching) and UEDGE (LLNL)

The workhorse tools for interpretive and predictive plasma transport simulation the last decade or more have been the 2-D edge and scrape-off layer fluid plasma simulation codes, UEDGE [54] and B2 [55]. Both codes can utilize either a built-in fluid model for neutral transport or couple to a comprehensive, Monte Carlo kinetic neutral transport code, such as EIRENE (FZJ)[56] (used with B2; the coupled system is known as SOLPS [57]) or DEGAS 2 [58]

(usually run with UEDGE in a non-iterative, post-processing mode). UEDGE and SOLPS are described in more detail in the Boundary Physics (chapter 4); DEGAS 2 (PPPL) is described in the MHD chapter (chapter 2).

The fluid plasma transport codes self-consistently solve equations for the density, parallel velocity, and temperature of all ion species, as well as the electron temperature. This capability will allow us to interpret experiments on impurity behavior and, as was discussed in Sec. 5.2.3, provide insight into how a viable continuous vapor shielding regime of operation might be established.

The characterization of particle sources and sinks at material surfaces in these codes resides within the neutral transport models. In the case of the built-in models, the level of detail and realism in these characterizations is limited. The Monte Carlo neutral transport codes provide a great deal more flexibility and very sophisticated models. Presently, the bulk of the data used to describe plasma-material interactions come from TRIM (or equivalent) and / or empirical expressions. We anticipate augmenting these models with data or fits obtained from more detailed and realistic MD simulations.

5.4.1.5.2 XGC-DEGAS2 (PPPL)

Limitations in the ability of fluid plasma-Monte Carlo neutral codes to reproduce aspects of tokamak scrape-off layer and divertor phenomena are well known. A common theme in virtually all of these assessments is that missing kinetic effects, particularly those associated with electrons in the scrape-off layer, are blamed. The XGC codes (chapter 4) will provide a closer to first principles model that will incorporate the missing kinetic effects and, presumably, more faithfully replicate experimental observations. Just as with the fluid plasma transport code, the XGC codes are being coupled to DEGAS 2 to allow detailed PMI models to be incorporated into the simulations.

5.4.1.5.3 OEDGE/DIVIMP (UTIAS)

An alternative approach to simulating scrape-off layer and divertor plasmas is a purely interpretive one. The OEDGE [59] code exploits the fact that our understanding of neutral and parallel plasma transport is vastly superior to that of anomalous, turbulence driven perpendicular transport. At the core of OEDGE is the Onion Skin Model (OSM) which integrates fluid plasma transport equations along individual SOL flux surfaces, starting from the divertor target and extending up to the main chamber, e.g., midplane. The initial plasma densities and temperatures at the divertor target are provided by measurements there, e.g., embedded Langmuir probes. Likewise, the results at the end points of the integration are to be compared with measurements made there, e.g., by a fast scanning probe.

By performing this integration on a set of adjacent flux surfaces, a full 2-D characterization of the SOL and divertor plasma can be compiled. This, in turn, can be used as the background for Monte Carlo neutral (the EIRENE code) and impurity (DIVIMP) transport codes. In addition to providing corresponding sources and sinks that can be fed back into OSM, analogous to the coupling in conventional fluid plasma-Monte Carlo neutral transport codes, the neutral and impurity codes also simulate relevant diagnostic signals, the data from which can be used to further constrain the calculations. The coupling and constraining process can then be iterated until a consistent solution is obtained.

OEDGE would be applied to the research thrusts described in this chapter in a manner similar to that used with the other codes described above.

5.4.1.6 1-D Modeling of Mixed-Material Films

For the "Material Migration" thrust (Sec. 5.2.2), a simpler, local approach to modeling the erosion and redeposition process is planned that can be developed and validated on the linear plasma device Magnum-PSI and then applied to NSTX-U. A particle balance equation for a thin film on the material surface is solved, incorporating contributions from redeposition, sputtering, evaporation, and diffusion. The redeposition term is computed via a semi-analytic, 1-D model characterization of neutral transport from the surface, ionization, and return to the surface. The ionization rates are obtained from the ADAS database. The associated photon emission rates can be compared with diagnostic measurements to infer the overall magnitude of the surface erosion. The surface sputtering rate can be computed using TRIM (or equivalent); direct experimental measurements will also be done. Evaporation rates (e.g., for Li) are well known. The diffusion of film atoms into the substrate is characterized with an empirically determined diffusion coefficient.

References

[1] "Materials science and technology research opportunities now and in the ITER era: a focused vision on compelling fusion nuclear science challenges" FESAC report, February 2012.
[2] F. Romanelli, et al., "A roadmap to the realization of fusion energy" presented at the 1st IAEA DEMO Programme Workshop, Los Angeles, 15-18 Oct. 2018.
[3] J.E. Menard, et al., Nucl. Fusion 52 (2012) 083015.
[4] Th. Eich, et al., "Scaling of the tokamak near scrape-off layer H-mode power width and implications for ITER", ITPA-Div/Sol group ITR 1/1, San Diego, October, 2012.
[5] J.E. Menard, et al., Nucl. Fusion 51 (2011) 103014.
[6] A. Capece, et al., "The effects of contamination by residual gases in NSTX on D uptake and retention in Li films", presented at the 54th APS-DPP meeting, Providence, RI, October, 2012; C.H. Skinner, et al., "Plasma Facing Surface Composition during NSTX Li Experiments", J. Nucl. Mater. (2013) Accepted for publication.
[7] M.J. Baldwin, et al., Nucl. Fusion. 42 (2002) 1318.
[8] R. Kaita, et al., "Comparison of H-Mode Plasmas Diverted to Solid and Liquid Lithium Surfaces" J. Nucl. Mater. (2013) Accepted for publication.
[9] R. Maingi, et al., Nucl. Fusion 52 (2012) 083001.
[10] M.A. Jaworski, et al., "Liquid Lithium Divertor Characteristics and Plasma-Material Interactions in NSTX High-Performance Plasmas", 24th IAEA Fusion Energy Conference, EX/P5-31, San Diego, October, 2012.
[11] M.A. Jaworski, et al., Fusion Engineering and Design 87 (2012) 1711-1718.
[12] M. Ono et al., Nucl. Fusion 52 (2012) 037001 and references therein.
[13] N. Itou et al., J. Nucl. Mater., 290-293 (2001) 281.
[14] H. Kugel et al., Phys. Plasmas 15, 056118 (2008).
[15] "Surface chemistry analysis of lithium conditioned NSTX graphite tiles correlated to plasma performance" C. N. Taylor, K.E. Luitjohan, B. Heim, L. Kollar, J.P. Allain, C.H. Skinner, H.W. Kugel, R. Kaita, A.L. Roquemore, R. Maingi submitted to Fusion Engineering and Design October 2012.
[16] "Deuterium Uptake in Magnetic Fusion Devices with Lithium Conditioned Carbon Walls" P S Krstic et al., submitted to Phys. Rev. Lett., (2012).
[17] C. N. Taylor et al., Rev. Sci. Instrum. 83 (2012) 10D703.
[18] H.W. Kugel, et al., Fusion. Eng. Des. 87 (2012) 1724-1731.
[19] P.C. Stangeby, J. Nucl. Mater. 415 (2011) S278-S283.
[20] S. Mirnov, S.V., Lazarev, V.B., J. Nucl. Mater., (2011) in press.
[21] C.H. Skinner, et al., J. Nucl. Mater. 363-365 (2007) 247-251.
[22] C. N. Taylor et al., Rev. Sci. Instrum. 83 (2012) 10D703.
[23] M.A. Jaworski, et al., Fusion. Eng. Des. 87 (2012) 1711-1718.

[24] M.A. Jaworski, et al., J. Nucl. Mater. (2013) in press.
[25] J.P. Allain and D.N. Ruzic, Nucl. Fusion, 42 (2002) 202-210.
[26] R.P. Doerner, et al., J. Nucl. Mater. 290-293 (2001) 166-172.
[27] P.C. Stangeby, "Plasma Boundary of Magnetic Fusion Devices" Institute of Physics Press, 2000.
[28] J.P. Allain, M.D. Coventry and D.N. Ruzic, J. Nucl. Mater. 313-316 (2007) 641-645..
[29] J.N. Brooks, et al., J. Nucl. Mater. 290-293 (2001) 185-190.
[30] G. De Temmerman, et al., Nucl. Fusion 51 (2001) 073008.
[31] T. D. Rognlien and M. E. Rensink J. Nucl. Mater., 290-293 (2001) 312.
[32] M.L. Apicella, et al., Plasma Phys. Control. Fusion 54 (2012) 035001.
[33] Evtikhin, V.A., et al., J. Nucl. Mater., 307-311, (2002) 1664-1669.
[34] T. Abrams, et al., J. Nucl. Mater. (2013) in press.
[35] C.S. Pitcher, P.C. Stangeby, Plasma Phys. Control. Fusion 39 (1997) 779.
[36] ADAS Database
[37] S. Mirnov, et al., Plasma Phys. Control. Fusion 48 (2006) 821.
[38] S. Loch, et al., Phys. Rev. E, 69 (2004) 066405.
[39] A. Hassanein and I. Konkashbaev, J. Nucl. Mater. 290-293 (2001) 1074-1078.
[40] J.N. Brooks, et al., J. Nucl. Mater. 290-293 (2001) 185-190.
[41] R. Neu, et al., Physica Scripta **T138** (2009) 014038.
[42] T. Willard, R. Vieira and S. Pierson, "Lamellae tungsten tile design transient thermal/ electromagnetic stress analysis" MIT PSFC internal report, Cambridge, MA, June 8, 2006.
[43] Ph. Mertens, et al., "Conceptual design for a bulk tungsten divertor tile in JET" Technical report EFDA-JET-CP(06)04-02, Sept. 2006.
[44] M.A. Jaworski, et al., "Liquid lithium divertor characteristics and plasma-material interactions in NSTX high-performance plasmas", submitted to Nucl. Fusion.
[45] W. Eckstein and D.B. Heifetz, J. Nucl. Mater. 145-147 (1987) 332.
[46] P. Krstic et al., Phys. Rev. Lett **110** (2013) 105001
[47] H. P. Summers (2004) The ADAS User Manual, version 2.6 http://www.adas.ac.uk
[48] T. Rognlien and M. Rensink, J. Nucl. Materials **290-293** (2001) 312
[49] A. *Pigarov* and S. Krasheninnikov, J. Nucl. Materials **390-391** (2009) 192
[50] J. R. Cary et al., J. Phys.: Conf. Ser. **125** (2008) 012040
[51] A. Pigarov et al., Cont. Plasma Phys. **52** (2012) DOI: 10.1002/ctpp.201210035
[52] K. Schmid et al., J. Nucl. Mat. **415** (2011) 284
[53] K. Schmid, EFDA TF-PWI Joint Working Session, Tervaniemi, Finland, February 2-6, 2013
[54] T. Rognlien et al., J. Nucl. Mater. **196–198** (1992) 347
[55] Braams B. J., "Computational studies in tokamak equilibrium and transport", Ph.D Thesis, Rijksuniversitet Utrecht (1986)
[56] D. Reiter et al., J. Nucl. Mater. **196–198** (1992) 241

[57] R. Schneider et al., J. Nucl. Mater. **196–198** (1992) 810
[58] D. Stotler and C. F. F. Karney, Plasma Phys. **34** (1994) 392
[59] P. Stangeby et al., Proc. 28th European Phys. Soc. Conf. Plasma Phys. Cont. Fusion, Madeira, Portugal, June 18–22, 2001
[60] F. Scotti, "Impurity sources and transport modification due to lithium wall conditioning in NSTX", 54th American Physical Society Division of Plasma Physics meeting, Providence, RI, October, 2012.

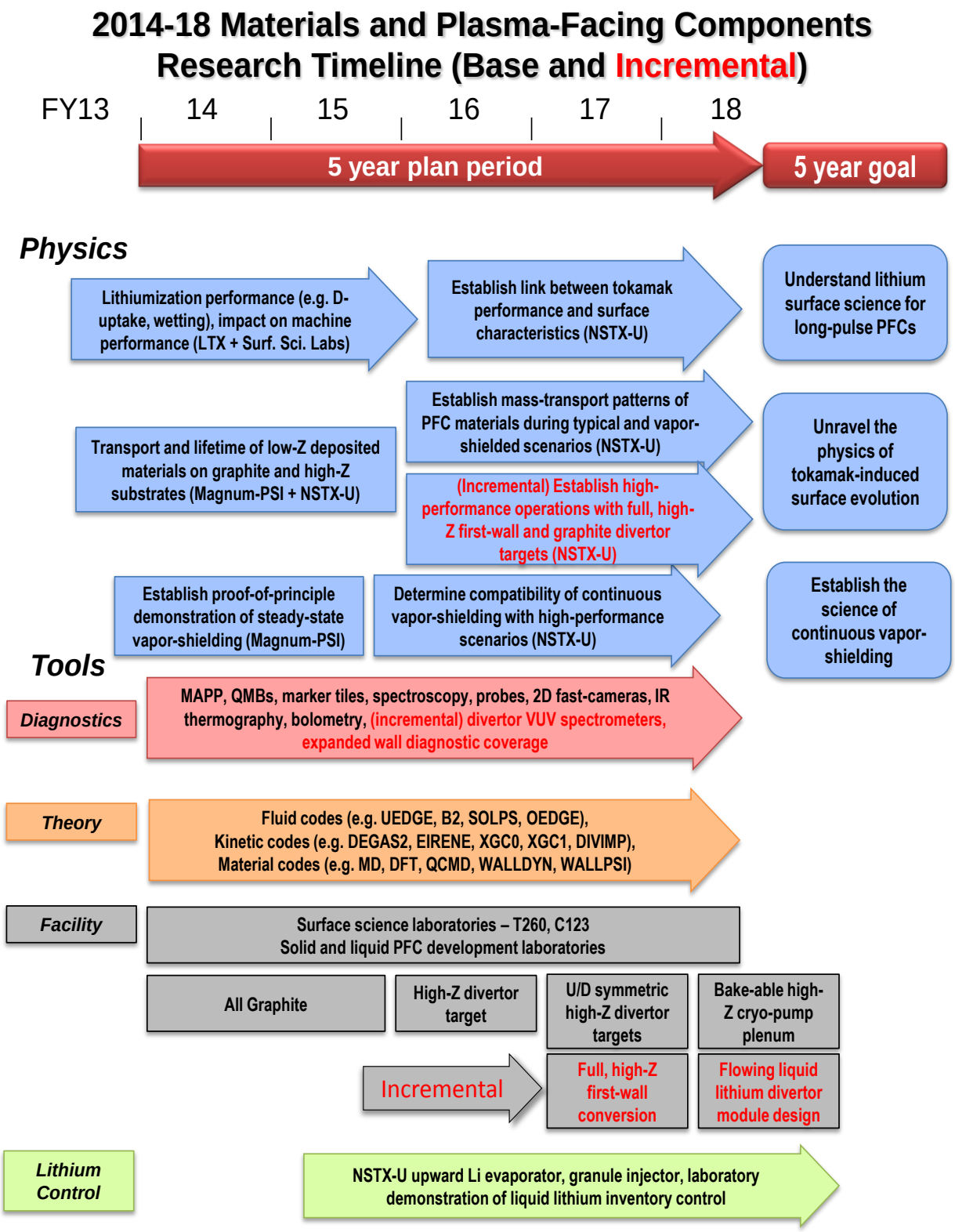
2014-18 Materials and Plasma-Facing Components Research Timeline (Base and Incremental)
FY13
14
15
16
17
18
5 year plan period
5 year goal
Physics
Lithiumization performance (e.g. D-uptake, wetting), impact on machine performance (LTX + Surf. Sci. Labs)
Establish link between tokamak performance and surface characteristics (NSTX-U)
Understand lithium surface science for long-pulse PFCs
Transport and lifetime of low-Z deposited materials on graphite and high-Z substrates (Magnum-PSI + NSTX-U)
Establish mass-transport patterns of PFC materials during typical and vapor-shielded scenarios (NSTX-U)
(Incremental) Establish high-performance operations with full, high-Z first-wall and graphite divertor targets (NSTX-U)
Unravel the physics of tokamak-induced surface evolution
Establish proof-of-principle demonstration of steady-state vapor-shielding (Magnum-PSI)
Determine compatibility of continuous vapor-shielding with high-performance scenarios (NSTX-U)
Establish the science of continuous vapor-shielding
Tools
Diagnostics
MAPP, QMBs, marker tiles, spectroscopy, probes, 2D fast-cameras, IR thermography, bolometry, (incremental) divertor VUV spectrometers, expanded wall diagnostic coverage
Theory
Fluid codes (e.g. UEDGE, B2, SOLPS, OEDGE),
Kinetic codes (e.g. DEGAS2, EIRENE, XGC0, XGC1, DIVIMP),
Material codes (e.g. MD, DFT, QCMD, WALLDYN, WALLPSI)
Facility
Surface science laboratories – T260, C123
Solid and liquid PFC development laboratories
All Graphite
High-Z divertor target
U/D symmetric high-Z divertor targets
Bake-able high-Z cryo-pump plenum
Incremental
Full, high-Z first-wall conversion
Flowing liquid lithium divertor module design
Lithium Control
NSTX-U upward Li evaporator, granule injector, laboratory demonstration of liquid lithium inventory control